Magnetic diagnostics

Ph. Moreau

09th December 2024

IIS2024
13th ITER International School
~Magnetic fusion diagnostics and data science~
December 9-13, 2024 Nagoya Prime Central Tower, Nagoya (Japan)

Dr Philippe MOREAU

French Alternative Energies and Atomic Energy Commission,
Institute for Magnetic Fusion Research

Working on WEST –
W Environment in Steady-state Tokamak (R=2.42m; a = 0.5m)

- **Current position:**
  - Head of plasma operation group
  - Tokamak commissioning manager
  - Head of Session Leader team

- **Background and skills:**
  - Tokamak operation
  - Plasma control
  - Diagnostics, magnetics (WEST, ITER, etc.)

philippe.jacques.moreau@cea.fr

Plasma confinement in tokamaks: A combination of magnetic fields

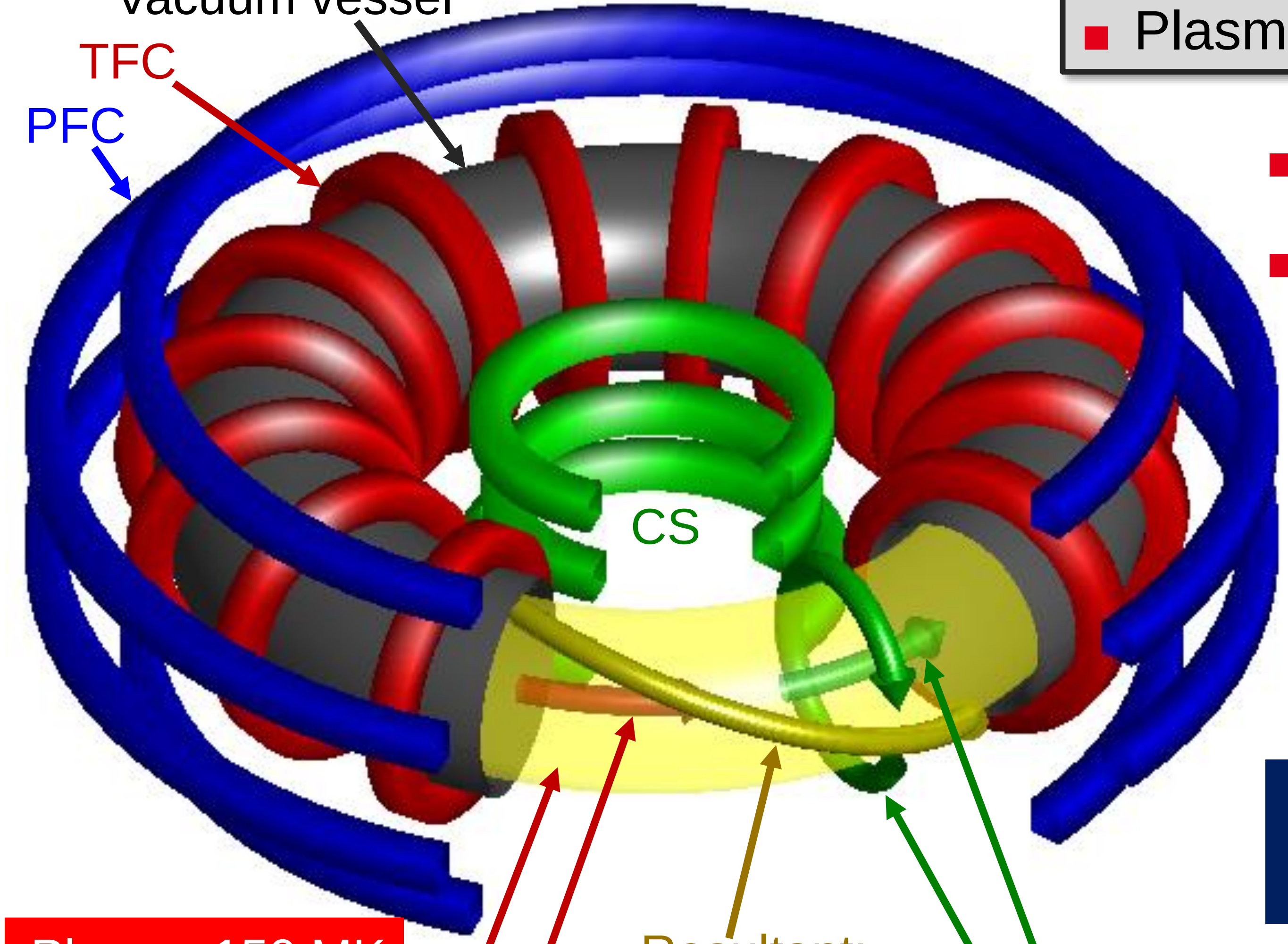

- Plasma confined in toroidal chamber with B fields

- Toroidal field
- Poloidal field

→ + → **Helical field lines**

- Tokamak: **central solenoid (CS)**
  → plasma current (transformer effect)

- **Poloidal field coils (PFC)**:
  → poloidal field → plasma position

Magnetic field, flux, are essential quantities and must be measured

Outline

1. **Magnetic fields and magnetic diagnostics in tokamaks**
2. **Magnetic sensors**
3. **Few hints about cabling**
4. **Signal conditioning: integrators**
5. **Equilibrium reconstruction and Real-Time data processing**

1. Basis about magnetic in tokamaks

Which magnetic field strength are we speaking about?

- Unit of magnetic field intensity is: Tesla (in honor of Nikola Tesla 1856 – 1943)
- Source are: - Permanently magnetized material
  - Electric currents

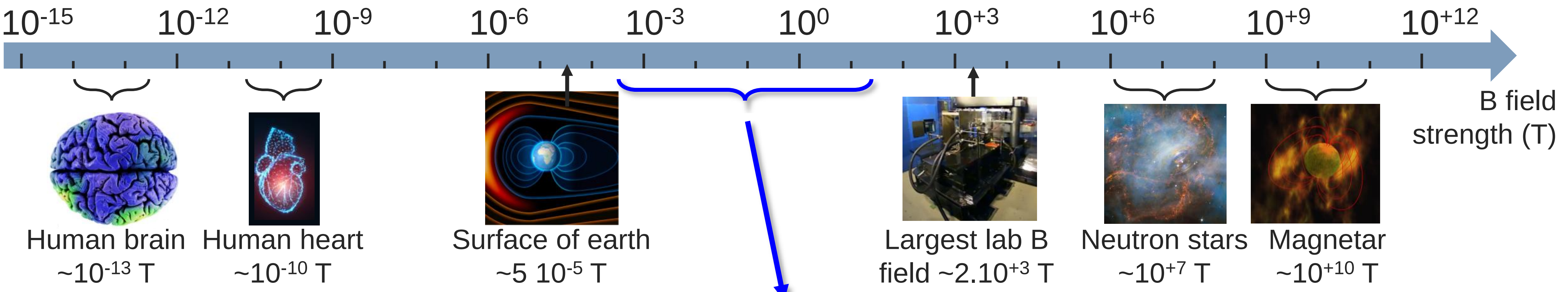

Permanent Magnet

Magnet on fridge ~10^{-3} T

Superconducting magnets 1-12 T

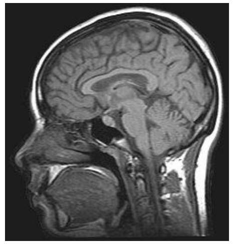

MRI (1-12T)

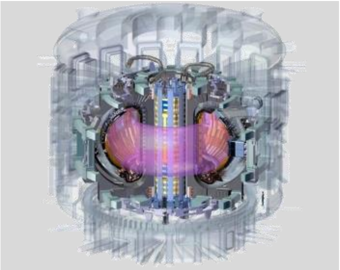

Fusion (<1mT - ~10T)

High energy physic (~8T)

A large diversity of magnetic sensors

- Types of sensors:
  - Inductive or steady state magnetic field measurements
  - **Vectorized** or total magnetic field measurements

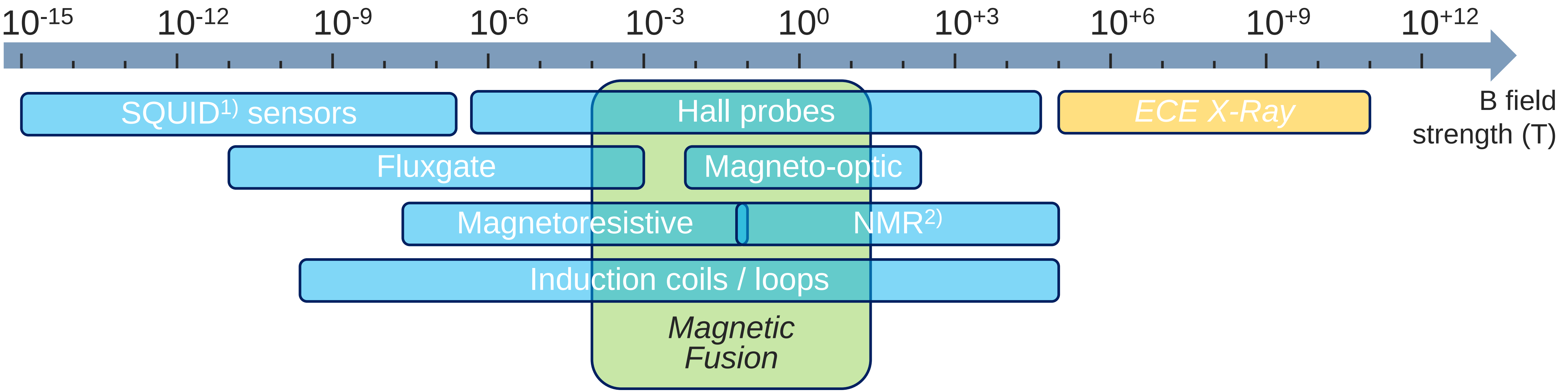

- **Selection of sensors requires taking into account the measurement constraints**

[1)] Superconducting Quantum Interference Device [2)] Nuclear Magnetic Resonance

Designing magnetic diagnostics

Constraints for future tokamaks (ITER)

Constraints existing on present day tokamaks

Diagnostic design

- Material selection
- Sensor design
- Sensor position
- Number of sensor (backup)
- Connection, joints design
- In-vessel cable routing

Constraints existing on present day tokamaks:

- Sensor sensitivity
- Sensor cut-off freq.
- Available volume
- Large temperature range (20-250°C)
- Deep vacuum ($<10^{-5}$Pa)
- No mainte-nance
- Many interfaces
- Diagnostic accuracy

Constraints for future tokamaks (ITER):

- Remote handling
- $\nabla T < 10°C$ in sensor
- Nuclear heating
- $\nabla T < 10°C$ along cable

Legend:

- Already on several tokamaks
- Poorly addressed up to Now. Few examples
- New issues. under inves-tigation. Requires R&D

<u>Available sensors:</u>

- Inductive coils/loops
- Hall probes
- Magneto-optic

<u>Disqualify:</u>

- Magnetoresistive, NMR (T°, neutrons)

Which information can be extracted from magnetic diagnostics?

Function	Parameter	Required measurement
Plasma equilibrium	Plasma current (Ip)	Rogowski coil B_{tang} B_{norm} Poloidal flux ψ
	Plasma position and shape	
	X-point position	
	dZ_p/dt	
	Loop voltage V_{loop}	
Diamagnetism	W_{dia}: Plasma energy	Toroidal flux variation $\delta\Phi_\phi$
MHD activity	Low frequency	HF sensors
	High frequency	

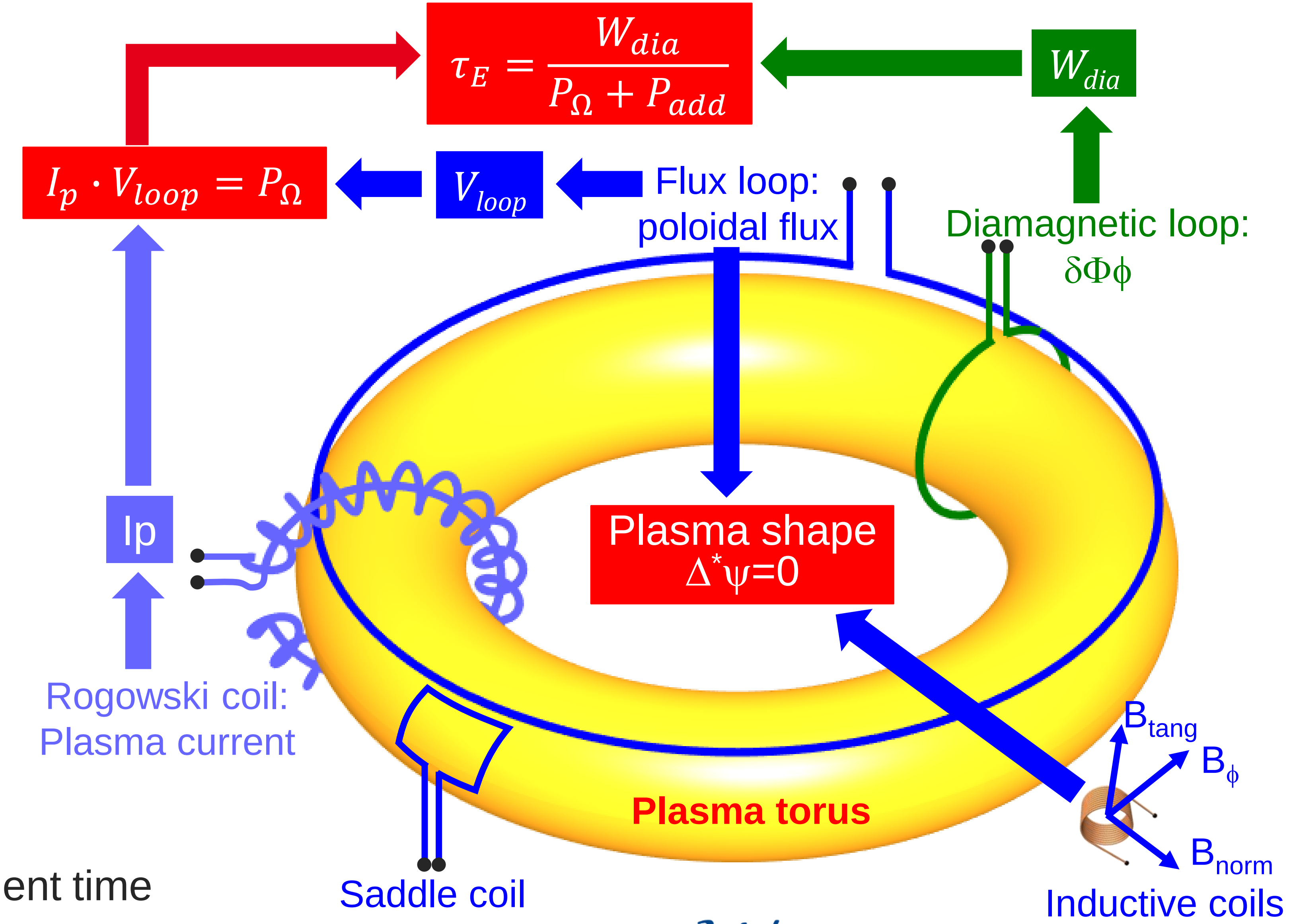

P_Ω = Ohmic power
τ_E = energy confinement time

Which sensor may satisfy the constraints and measurement accuracy ?

Function	Parameter	Required measurement
Plasma equilibrium	Plasma current (Ip 0 – 20 MA)	Rogowski coil B_{tang} B_{norm} Poloidal flux ψ
	Plasma position and shape	
	X-point position	
	dZ_p/dt	
	Loop voltage V_{loop}	
Diamagnetism	W_{dia}: Plasma energy	Toroidal flux variation $\delta\Phi\phi$
MHD activity	Low frequency	HF sensors
	High frequency	

- Two families of magnetic sensors:
  - Inductive: measure B variation vs time dB/dt
  - Non inductive: direct B measurement

	Inductive sensors	Non-inductive sensors
Magnetic field vector	Induction coils (Mirnov coils)	Hall probes
Magnetic flux (toroidal and poloidal)	Flux loops	
Current measurement	Rogowski coils	Magneto-optic (Fiber Optic Current Sensor)

From the sensor to the acquisition

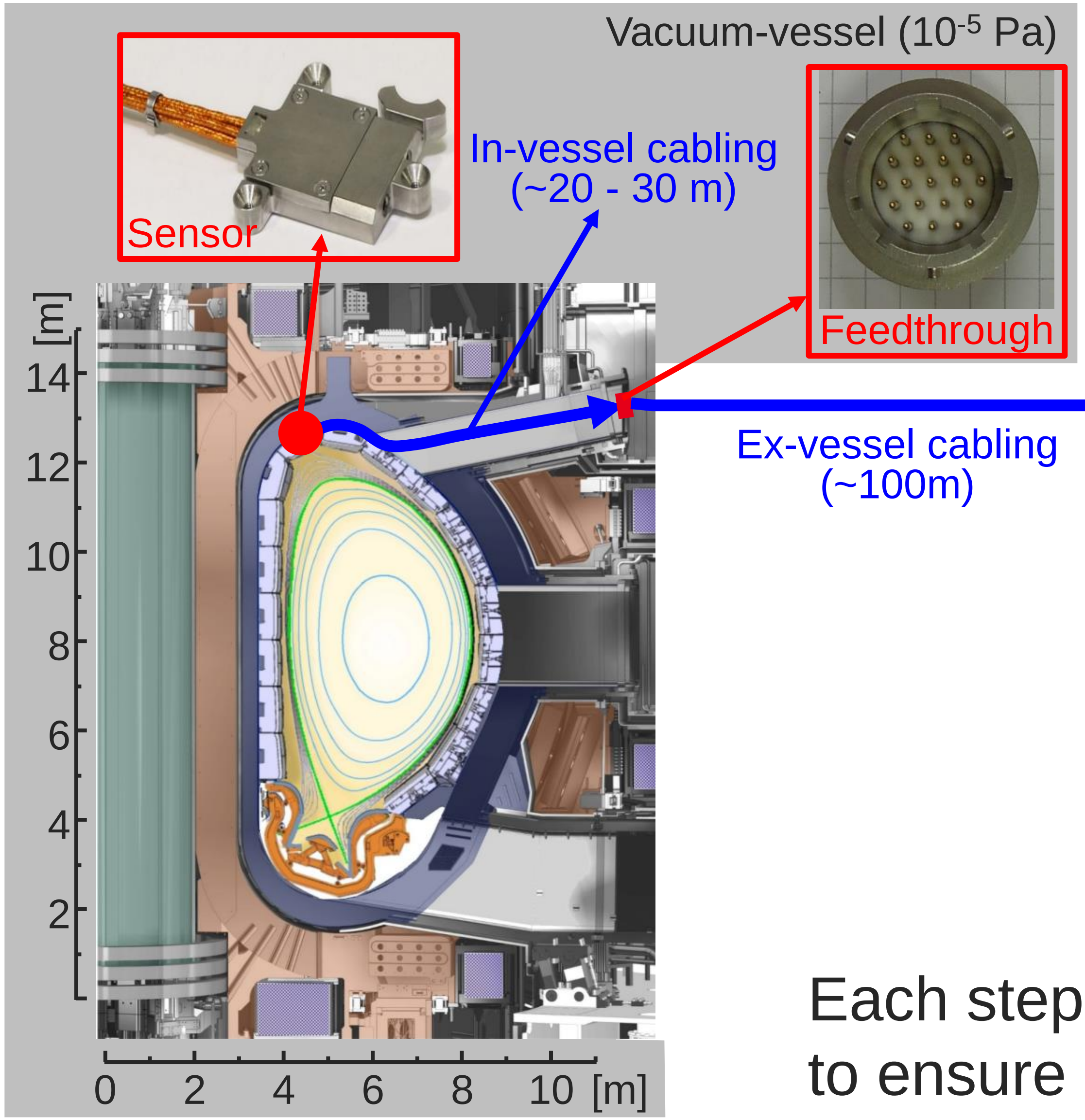

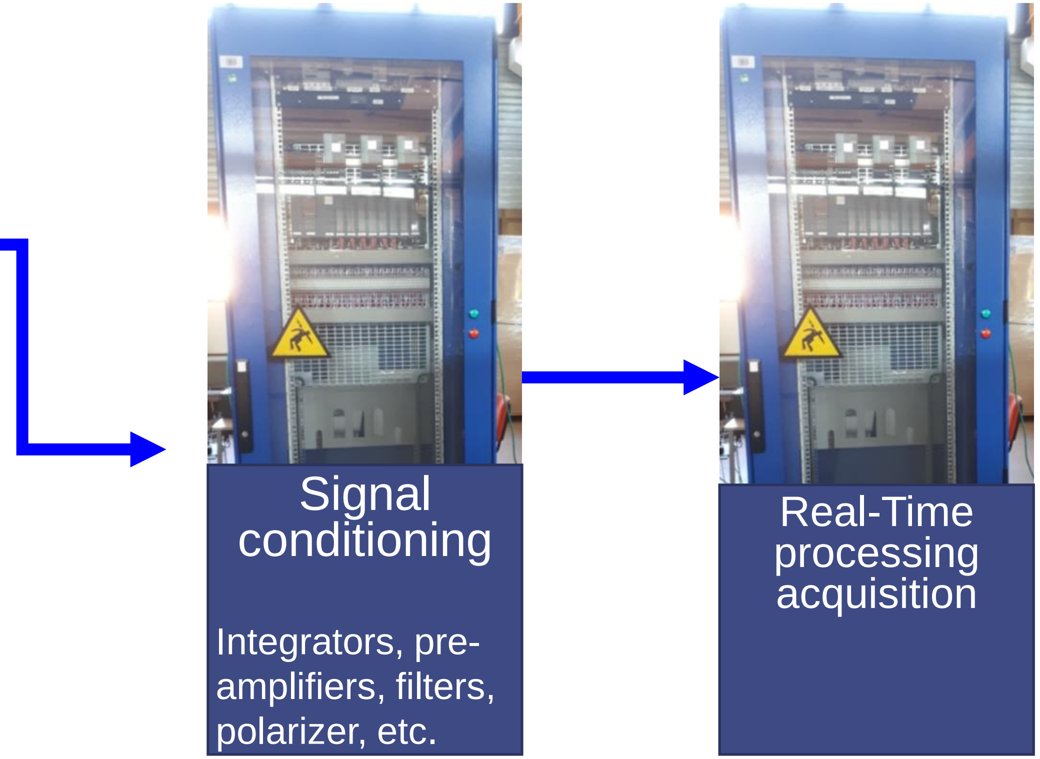

Each step of the measurement chain is important to ensure the diagnostic accuracy

2. Magnetic sensors

2.1. Magnetic field and flux measurements

→ Plasma equilibrium

Local $\vec{B}$ measurement: Induction coils or mirnov coils

- Applications: measure 3D local magnetic field vectors → **plasma equilibrium**
- Measurement principle: Coil is a copper wire wound on a mandrel (e.g. cylinder)

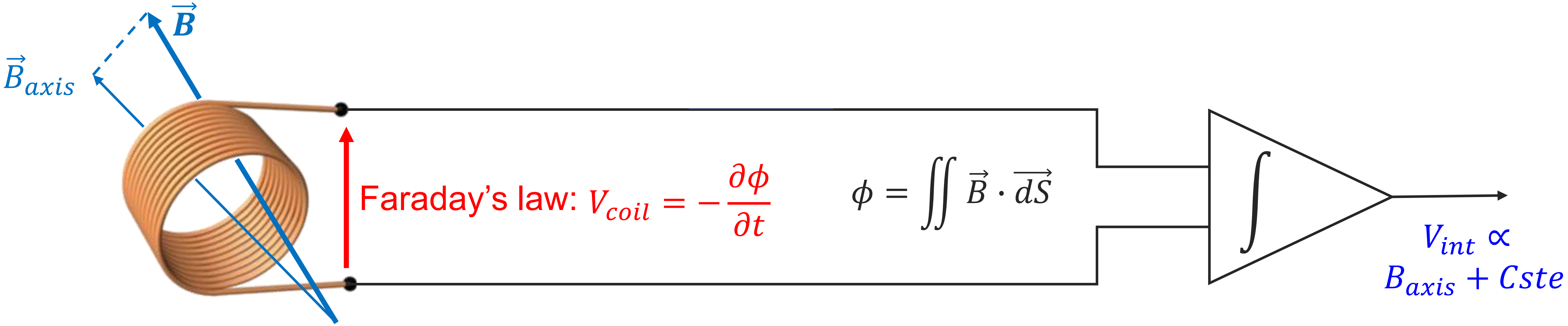

Small sensor ➔ uniform B crossing the winding $\phi = S\,\vec{B}_{axis}$ S is the coil effective area (m²)

$$V_{coil} = -S\,\frac{\partial B_{axis}}{\partial t}$$ Integration → $$\boldsymbol{V_{int} \propto B_{axis} + Cste}$$

Local $\vec{B}$ measurement: Induction coils or mirnov coils

- Advantage
  - Flexible design (accommodate geometry)
  - Sensitivity, cut-off freq. (#layers, #turn/layer) set by design
  - Robustness
  - Simplicity of operation
- Shortcomings:
  - Inductive sensor (only sensitive to AC field)
  - Requires integrator electronic
  - Rather difficult to miniaturize.
    Nevertheless thin film technic are available LTCC(*)

(*) Low Temperature Co-Fired Ceramic

Mirnov coils for application on WEST

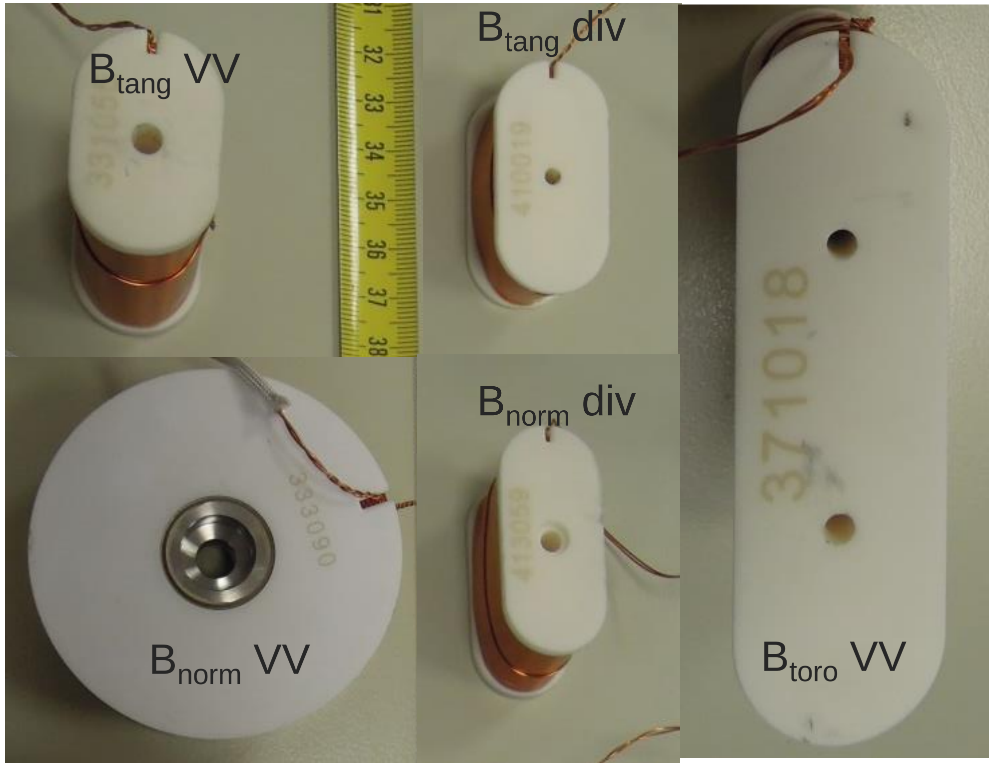

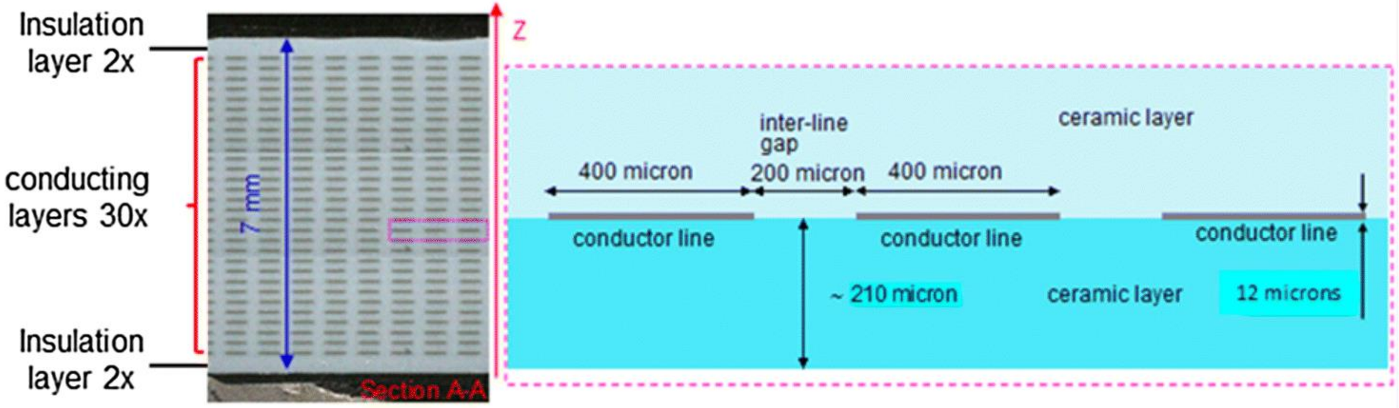

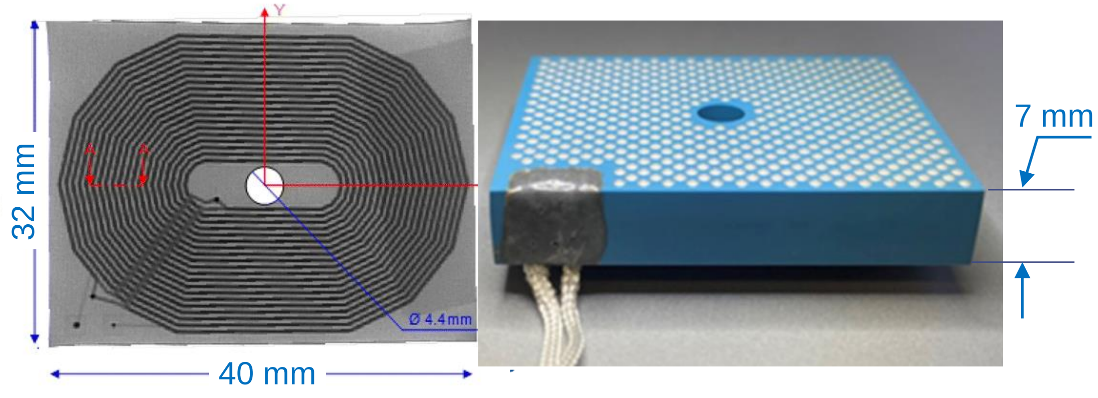

Local $\vec{B}$ measurement: Hall probe

- Applications: measure 3D local magnetic field vectors → **plasma equilibrium**
- Measurement principle: hall effect (emf created across conductor when current and magnetic field are present)

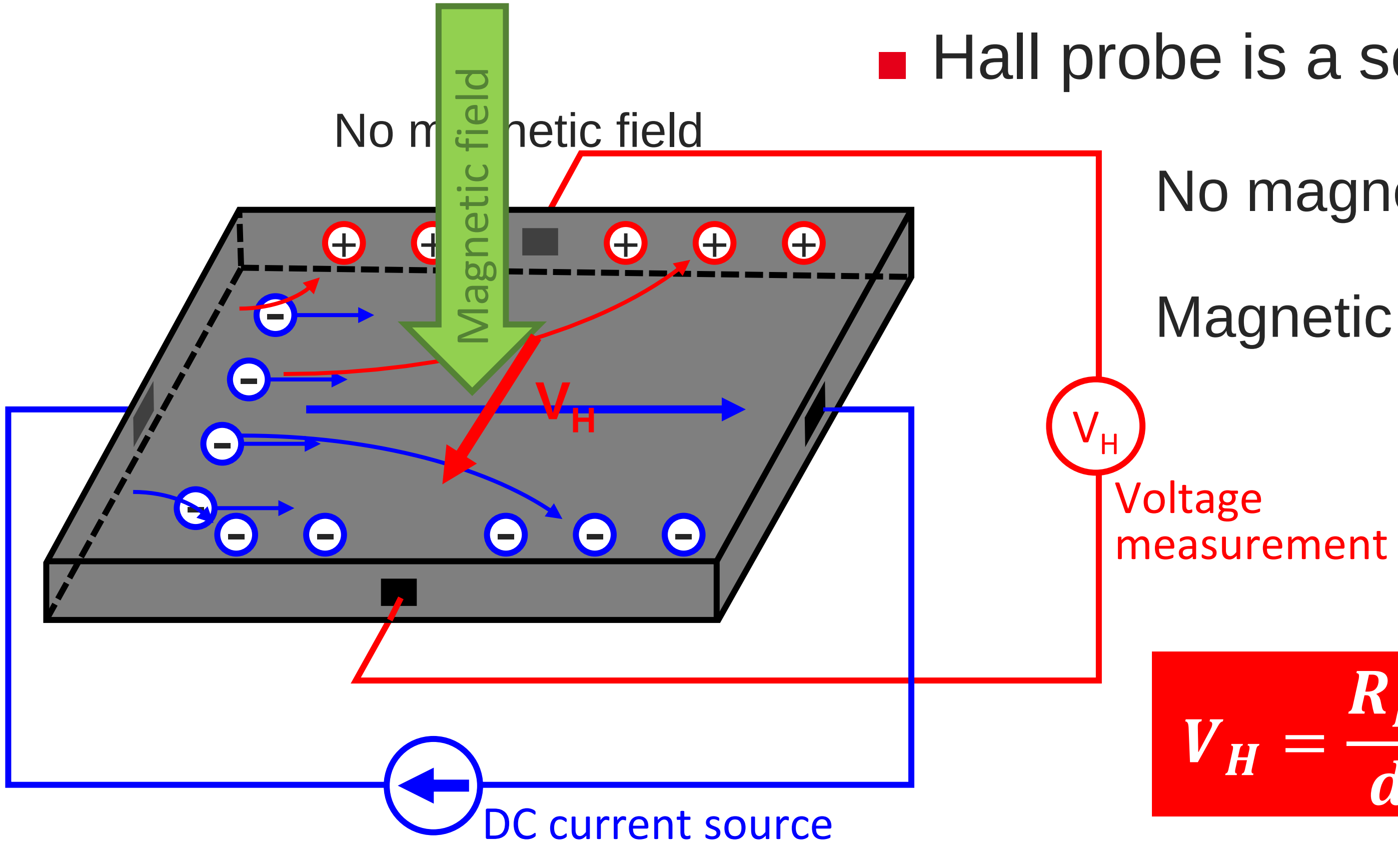

- Hall probe is a semiconductor (e.g. Si, GaAs, InSb, …)

No magnetic field ➔ electrons move straight, V=0

Magnetic field ➔ electrons movement deflected

🡇

More electrons present on one side

🡇

Electric field (voltage) develop ⊥ to B

$$V_H = \frac{R_H}{d} I B$$

R_H : fixed depend on HP material
d : thickness of the HP

Local $\vec{B}$ measurement: Hall probe

- Advantage
  - Most widely used magnetic sensor
  - Direct measurement of $\vec{B}$: $V_H = \frac{R_H}{d}\, I\, B$
  - Can be miniaturized
  - 3D measurements easy to implement
  - Low cost

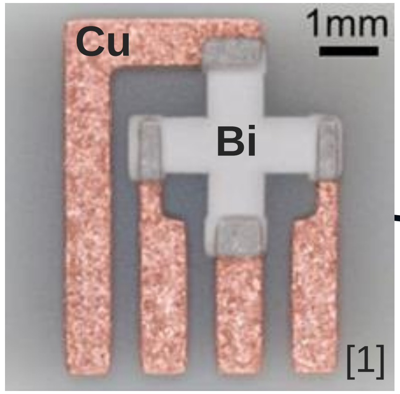

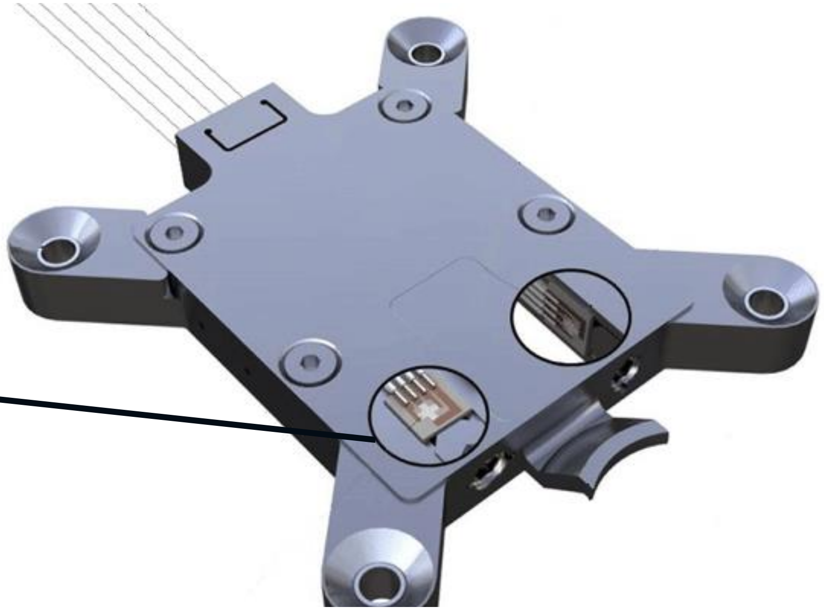

- Shortcomings:
  - Low sensitivity, V_H small, care necessary to avoid pick-up
  - More complex cabling than a simple induction coil (more wires)
  - Response depends on temperature (compensation needed)
  - Sensitive to neutrons efficiency decrease → regular recalibration

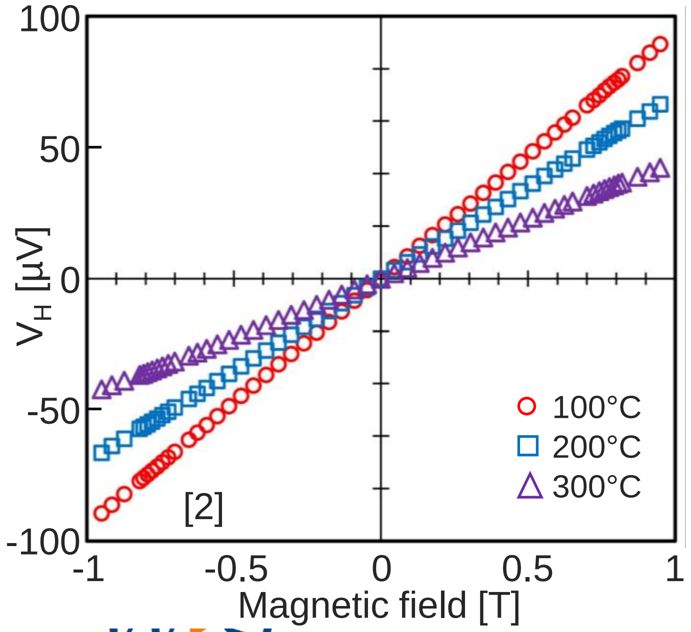

[1] https://doi.org/10.1063/1.5038871
[2] https://doi.org/10.1016/j.fusengdes.2023.113476

40 mm

2.2. Currents and plasma current measurements

Current measurement: Rogowski coil

- Applications: measure current linked by the Rogowski → **plasma current I_p**, halo current (plasma ↔ vessel), eddy currents, etc.
- Measurement principle: Cu wire wound as a spiral **+ return cable**. Installed around conductor

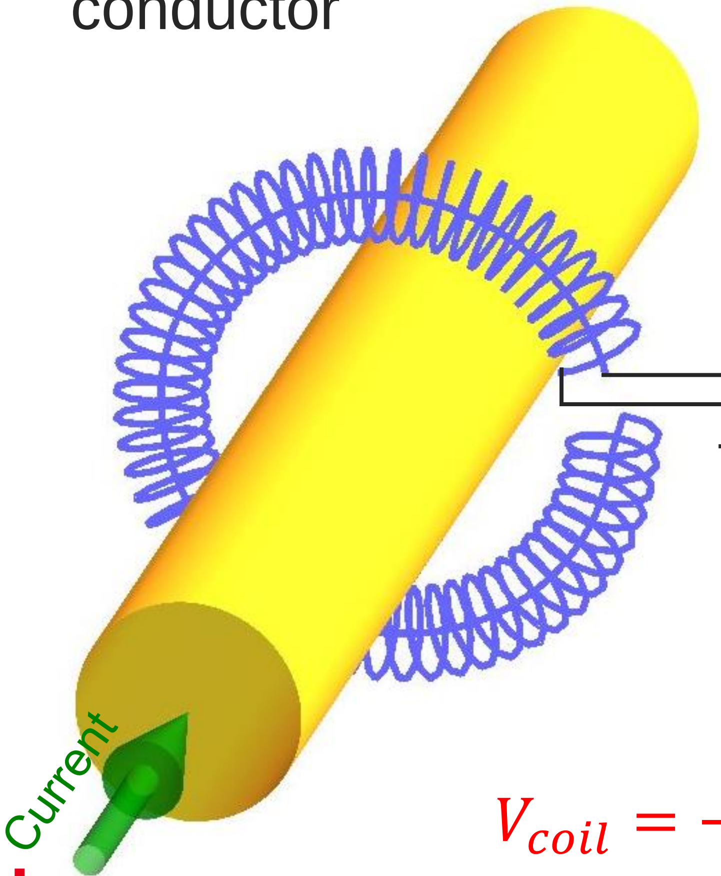

Faraday's law: $V_{coil} = -\frac{\partial \phi}{\partial t}$

Ampere's law: $\oint_{\partial\Sigma} \vec{B} \cdot d\vec{l} = \mu_0 \, I$

$\int$

$V_{int} \propto I + Cste$

Turn area A and pitch n determine the sensitivity

$$\phi = A\, n \underbrace{\oint \vec{B} \cdot \vec{dl}}_{Ampere's\ law} = A\, n\, \mu_0\, I$$

A = area of 1 turn;
n = number of turn per meter

$$V_{coil} = -A\, n\, \mu_0 \frac{\partial I}{\partial t}$$

Integration →

$\boldsymbol{V_{int} \propto I + Cste}$

Current measurement: Rogowski coil

- Wound on the inner skin of the VV, a Rogowski measures Ip

- Advantage
  - Routing is free (Ampere's law) → Flexible design
  - Compactness, Robustness
  - Simplicity of operation

- Shortcomings:
  - Inductive sensor (only sensitive to AC field)
  - Requires integrator electronic
  - Requires perfectly uniform winding
    → in any case pick-up from outer Rogowski current must be taken into account (calibration)

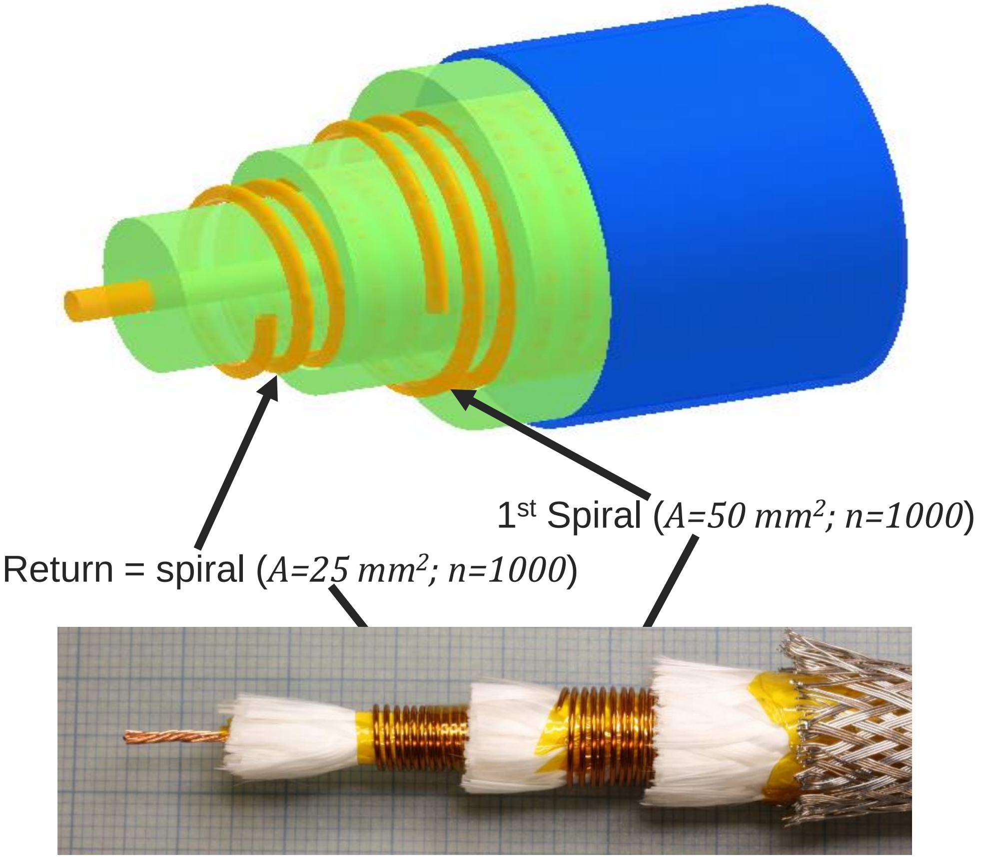

ITER External Rogowski design

40 mm

Current measurement: Fiber Optic Current Sensor

- <u>Applications:</u> measure current linked by the fiber optic → **plasma current I_p**, halo current (plasma ↔ vessel), eddy currents, etc.
- <u>Measurement principle:</u> Faraday rotation of light polarization due to magnetic field

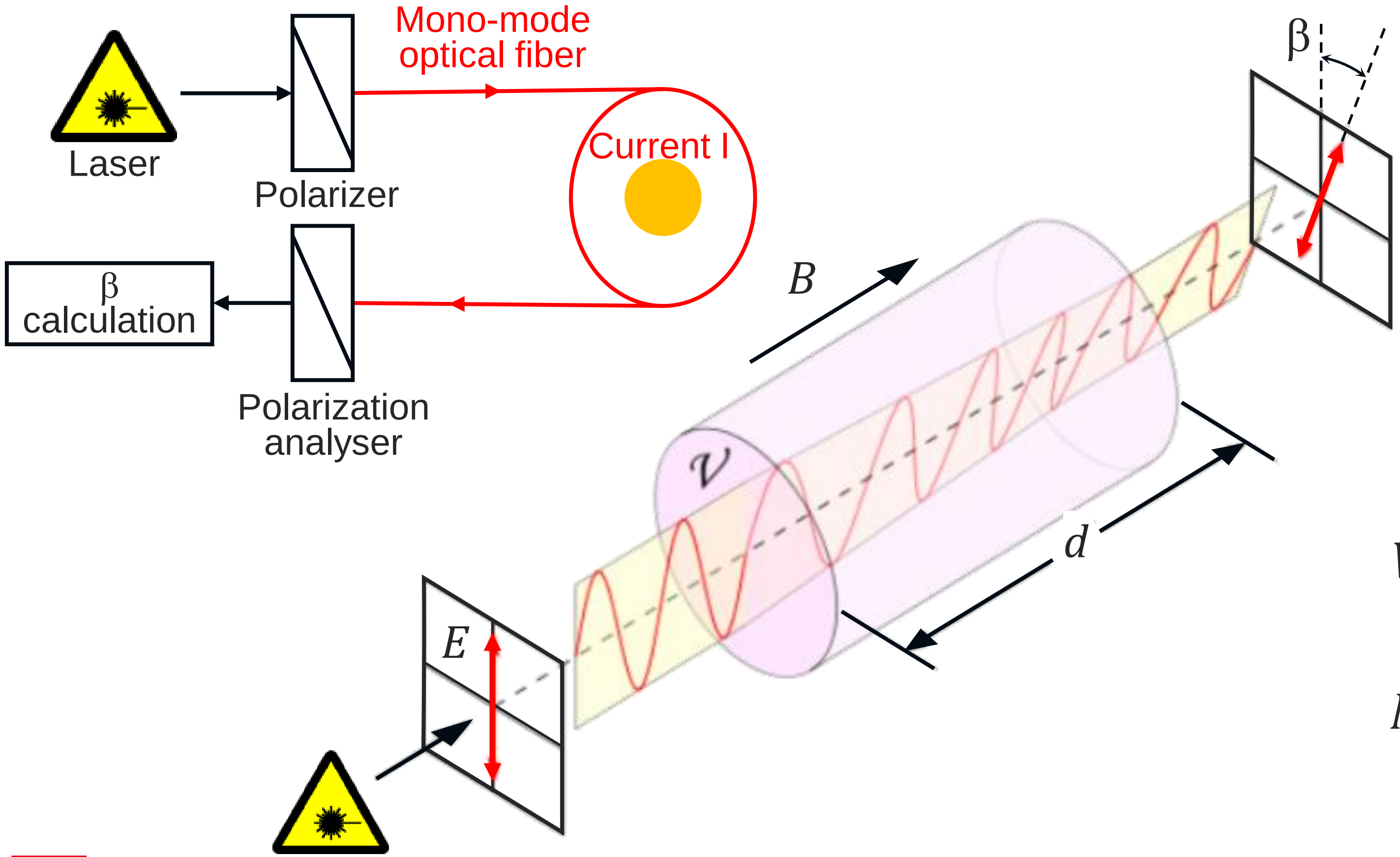

Faraday Effect in optical fiber:

$$\beta = N\,V \underbrace{\oint \vec{H}\cdot\vec{dl}}_{Ampere's\ law} = N\,V\,I$$

V = Verdet constant of optical fiber
V ~ 0.71 rad/MA @ λ=1550 nm

N = number of turns around the conductor

Current measurement: Fiber Optic Current Sensor

- Wound on the inner skin of the VV, FOCS measures Ip.
  Also used in the industry to measure large current

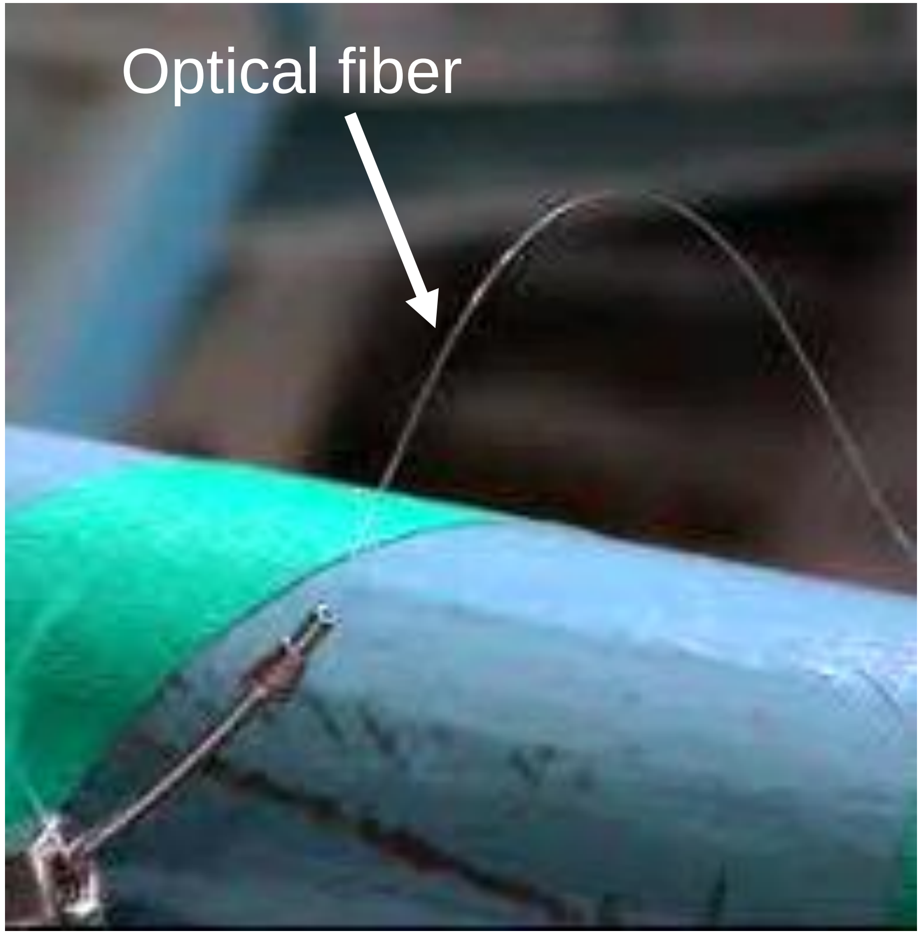

- Advantage
  - Direct measurement of current (not current variation): $\beta = N\,V\,I$
  - Routing is free (Ampere's law) → Flexible design
  - Compactness, Robustness
  - Replaceable (blowing technics exist)

- Shortcomings:
  - Spurious effects (non linear birefringence) must be considered
    Measurement interpretation might be complex
  - Higher cost than just an induction coil
  - Sensitivity much smaller than inductive coils (but OK for ITER)

Current measurement: Other technics

- "partial Rogowski" = several tangential field coils around the VV

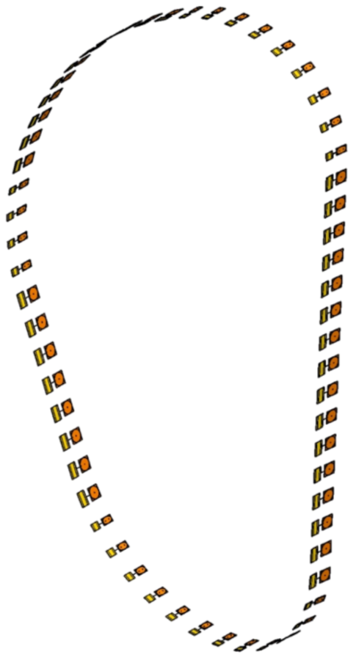

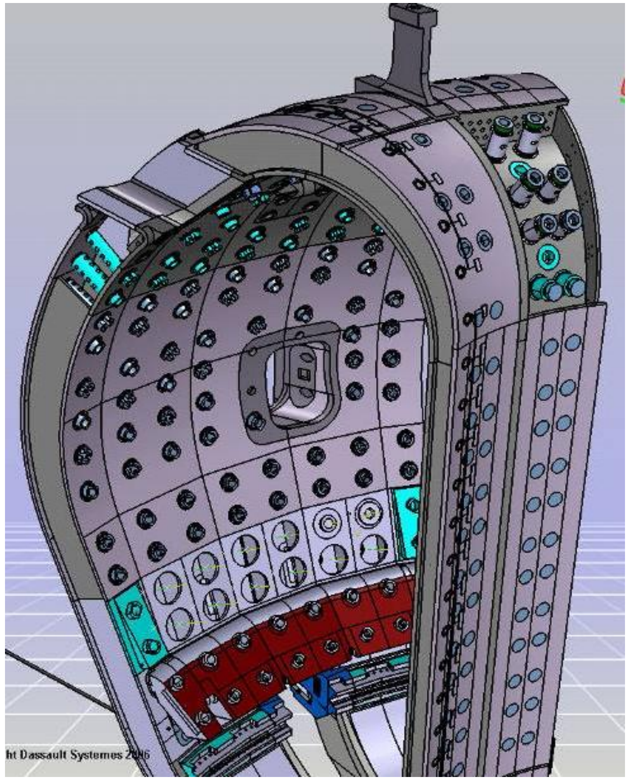

Current = weighted sum of B_{tang} $$I_p = \sum_i \alpha_i \, B_{tang\_i}$$

- "Resistive Shunt" = Voltage drop through a known resistance plugged on 2 points of an electrical circuit

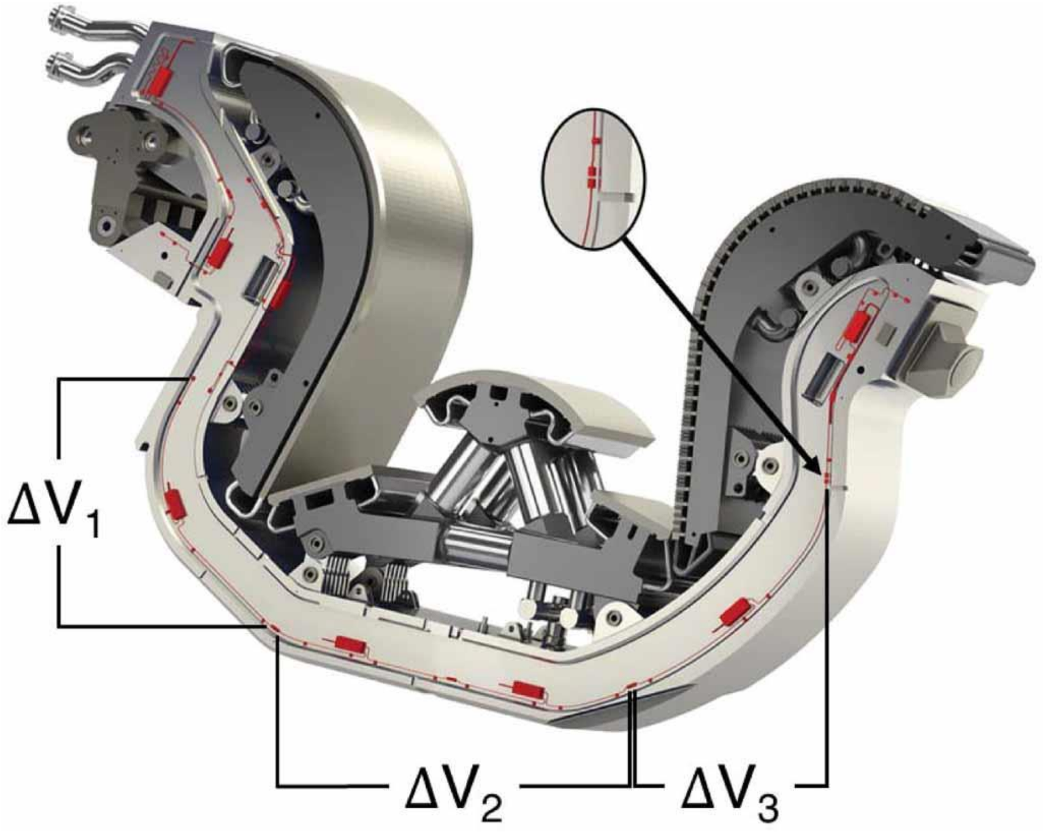

2.3. Loop voltage and flux measurements

Loop voltage and flux: Flux loop

- <u>Applications:</u> measure loop voltage, plasma flux and diamagnetic flux.
- <u>Measurement principle:</u> Voltage induced in a loop of cable (Faraday's law)

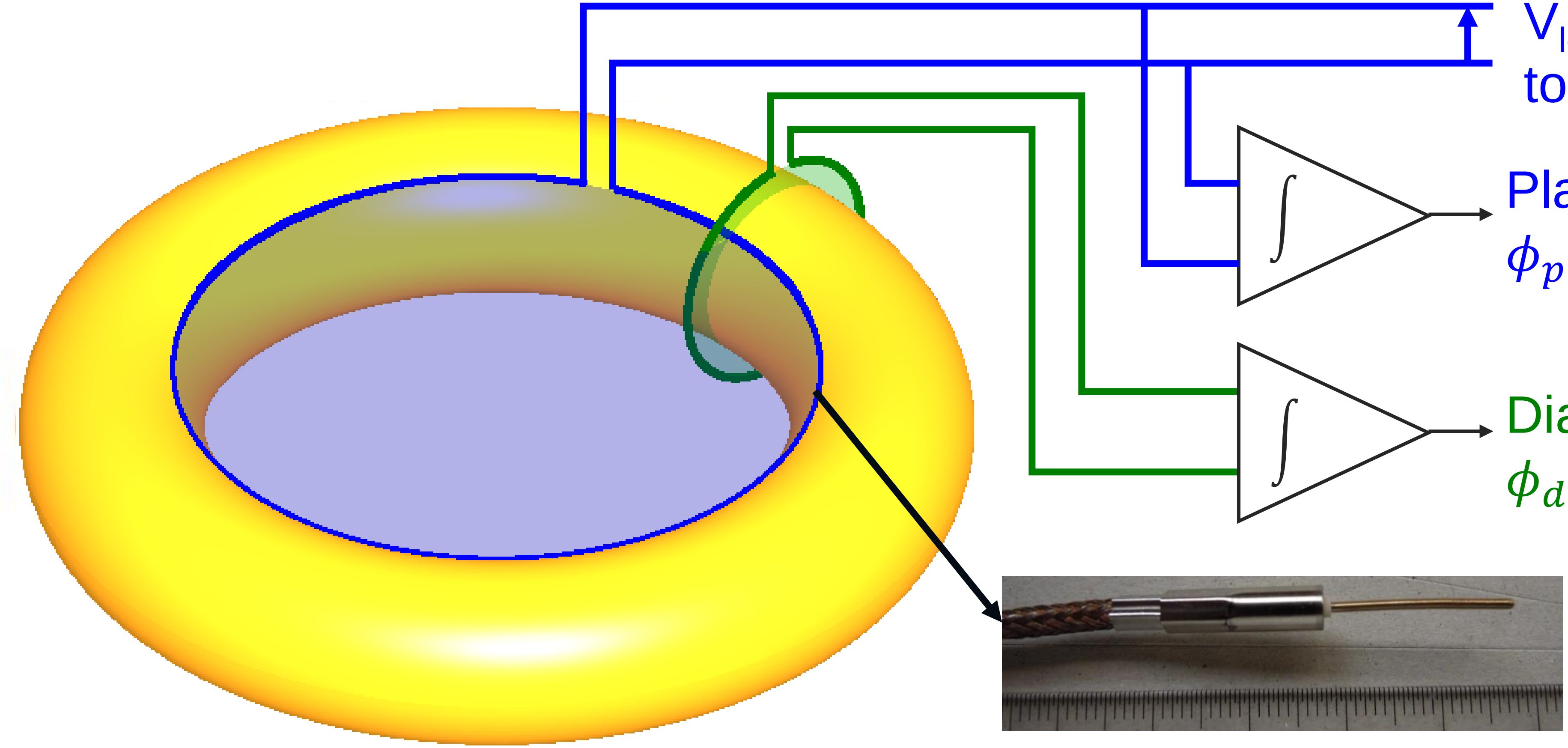

V_{loop}~ Electric field applied to plasma torus

Plasma flux → equilibrium

$\phi_{plas} = \int V_{loop} dt$

Diamagnetic flux

$\phi_{diam} = \int V_{diam} dt$

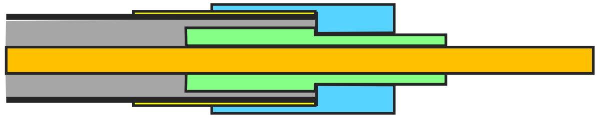

Flux loop cable and terminal

2.4. Fast fluctuations in the equilibrium magnetic field

→ MHD Instabilities

HF $\vec{B}$ measurement: Induction coils or mirnov coils

- Applications: HF magnetic field → MHD
- Electric model of an induction coil

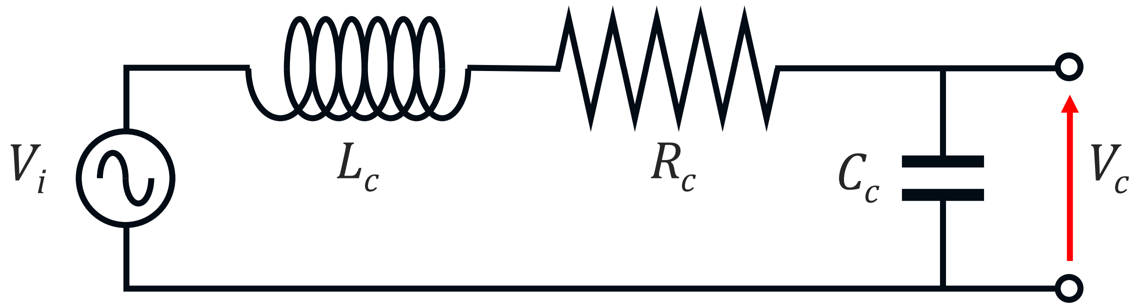

- Transfer function $H_p = \frac{V_c}{V_i}$ with $V_i = jS\omega B_{axis}$

$$\boldsymbol{H_p = \frac{S}{1 + j\omega\tau_c - \omega^2\tau_c\tau_p}}$$

$\tau_c = R_c\, C_c\ ;\quad \tau_p = \frac{L_c}{R_c}$

S = sensor effective area

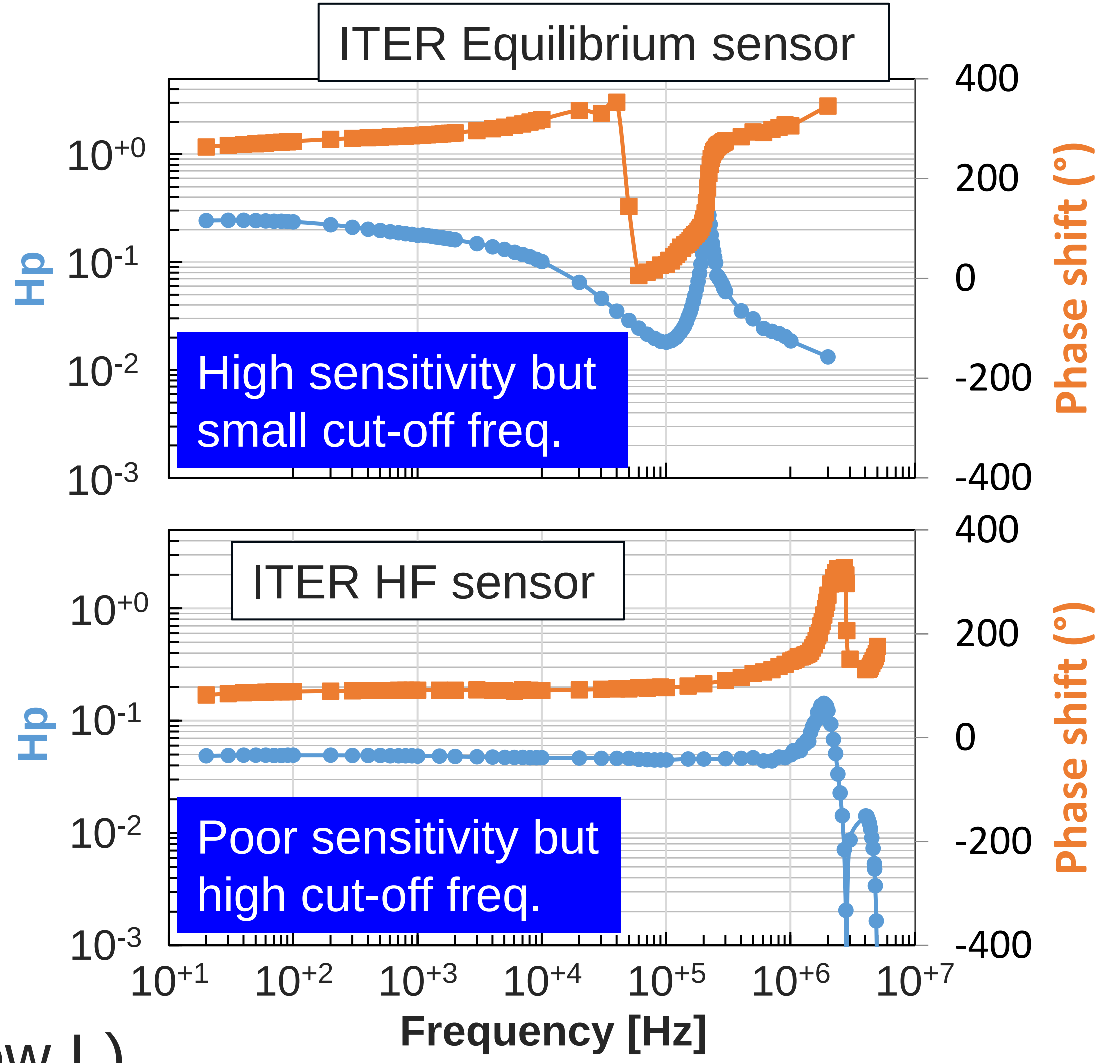

- Frequency response is a trade off between sensitivity (eff. Area) and cut-off frequency (low L)

3. Few hints about cabling

Sensor cabling

- Twisted pairs of cable mandatory

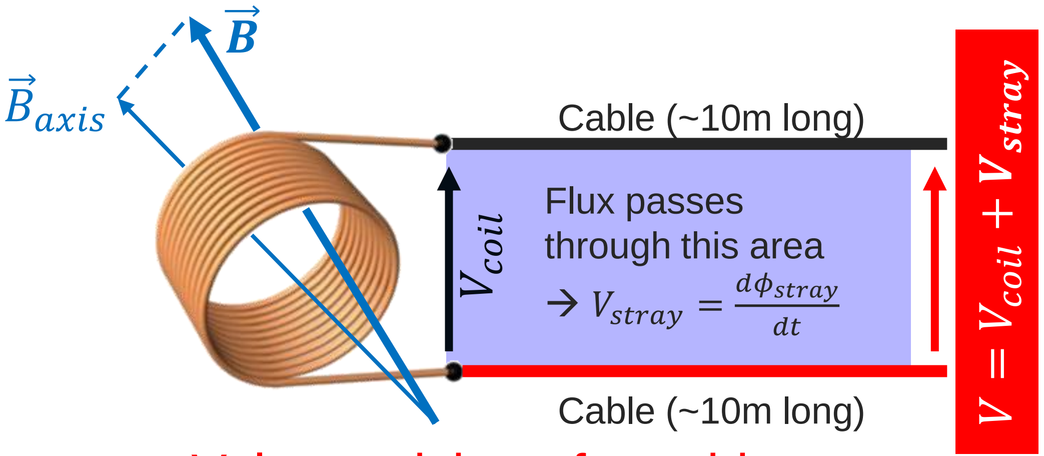

Voltage pick-up from this stray area

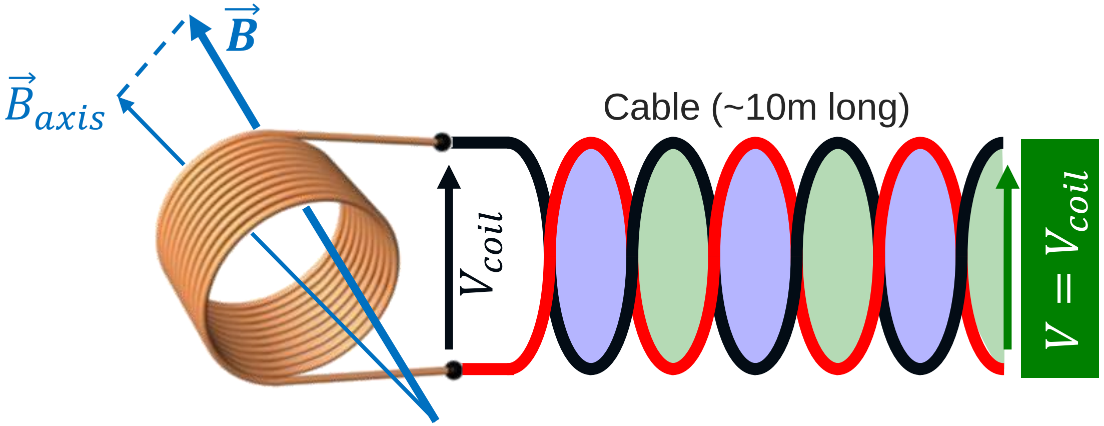

Twisted pair of cable → stray area cancellation

- Radiation hard cable and optic fiber

Wide type of effects induced by radiations:

- RIEMF: Radiation Induced Electro-Motive Force
- RIC: Radiation Induced Conductivity,
- TIEMF: Thermal Induced Electro-Motive Force
- RITES: Radiation induced Thermo-Electric Sensitivity, etc.
- RIA: Radiation Induced Absorption

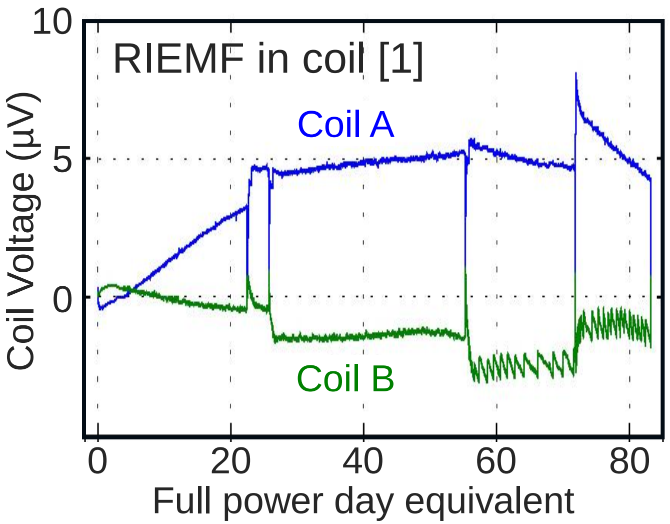

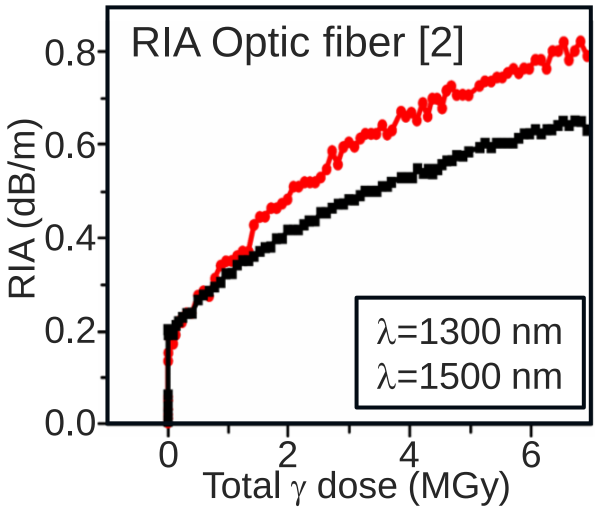

Spurious voltage 10µV leads to unacceptable error of 5% after 500s

[1] G. Vayakis et al. https://doi.org/10.1063/1.1787580
[2] B. Brichard, "Initial assessment of optical fibres as current sensors: gamma radiation effects", *EFDA TW5-IRRCER-Deliverable 9*

Sensor cabling

- The mineral insulated cables: twisted Cu cable + Stainless steel (or Cu) jacket. Electrical isolation done by inorganic

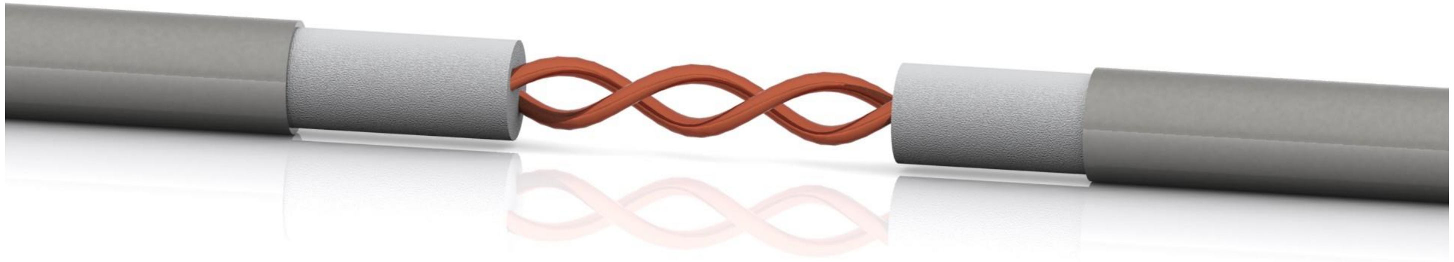

What ITER magnetic diagnostics look like?

- Mag. Diag. embedded in tokamak structure → No maintenance
- Radiation risk → additional sensor

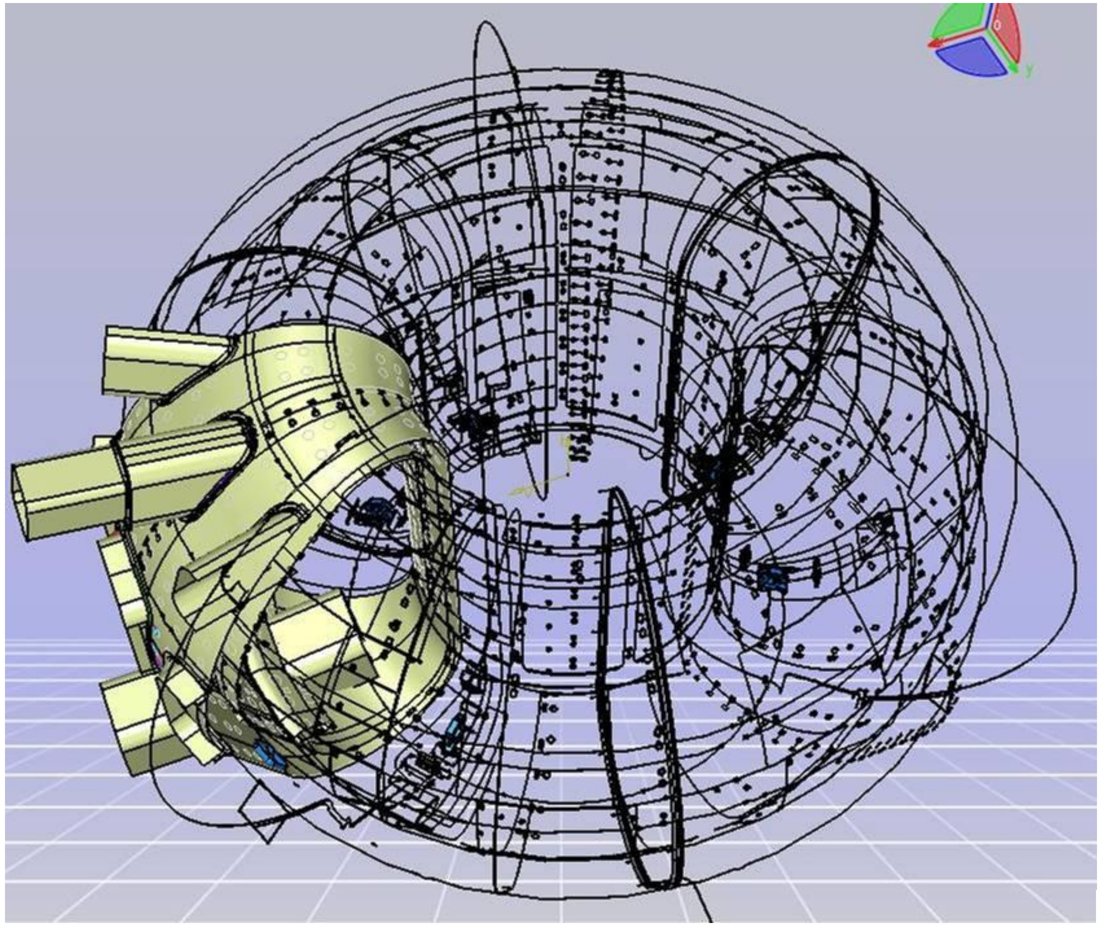

	Radiation / Dose (cm^{-2} s^{-1}) / MGy			
Location	n	γ	Type	Number
In-vessel sensors: Behind blanket modules, fixed on VV inner skin	$3.\ 10^{12}$ 500	10^{12} 340	Pick-up coils	186
			Rogowski (I_{halo})	360
			Flux loops	220
	10^{13} 1700	$3.\ 10^{12}$ 1000	HF coils	>300
Divertor	10^{13} 1700	$3.\ 10^{12}$ 1000	Pick-up coils	72
			Rogowski (I_{halo})	48
Ex-vessel sensors Fixed on VV outer skin	$1.5\ 10^{10}$ 2.5	10^{10} 3.4	Pick-up coils	360
			Steady state sensors	120
			Flux loops	5
			Optic fibre	12
Inside TFC case (T=4K)	$1.\ 10^{10}$ 1.7	$2.\ 10^{9}$ 0.7	Rogowski (I_p)	≥ 3

Total : ~ 2000 sensors, 19 types, >300km of cable

4. Signal conditioning: Integrators

Electronic: Integration of inductive sensor signal

- Signal from inductive coil: $V_{coil} = -S\,\frac{\partial B_{axis}}{\partial t}$ → B_{axis} obtained by integration of V_{coil}.
- The most simple active integrator circuit

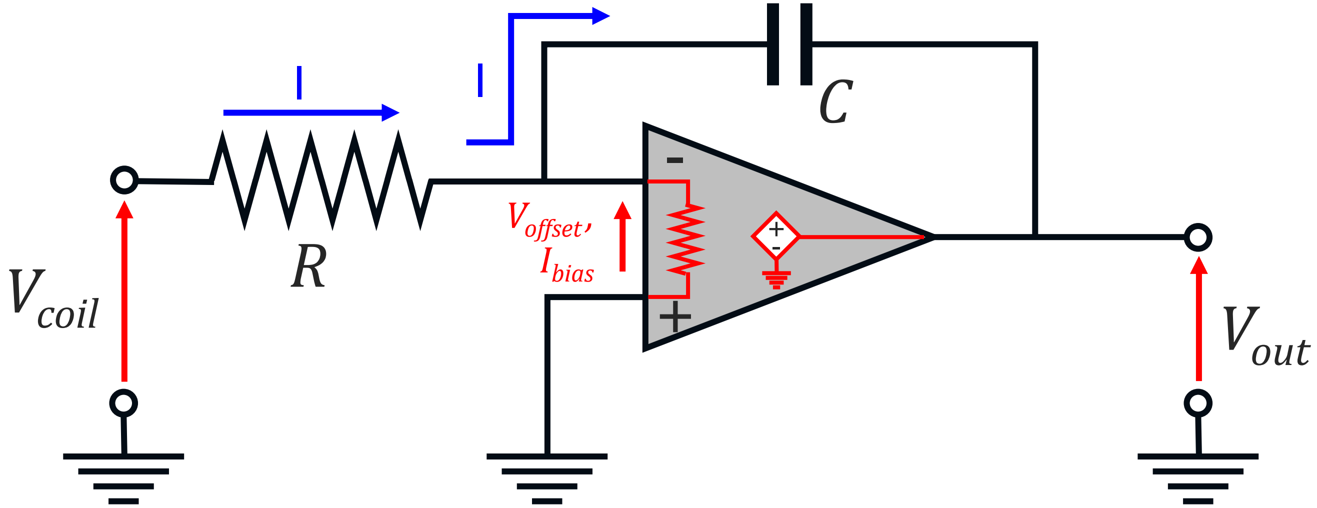

$$V_{out}(t) = -\frac{1}{\tau}\int_0^t V_{coil}\,dt + Cste$$

$$V_{out}(t) = \frac{S}{R\,C}\,B_{axis}(t) + B_{axis}(t=0)$$

- Must measure high freq. (start-up, disruption, etc.) and low freq. (current plateau) !
- Neither operational amplifier nor capacitor are ideal (V_{offset}, I_{bias}, current leaking, etc.) Spurious signal ~µV and ~nAmp

→ **Such simple integrator <u>DO NOT</u> work for fusion applications**

Integrators: Key is to compensate from spurious signal

- Almost all tokamaks have made their own developments

- Analog integrator e.g. WEST [1]

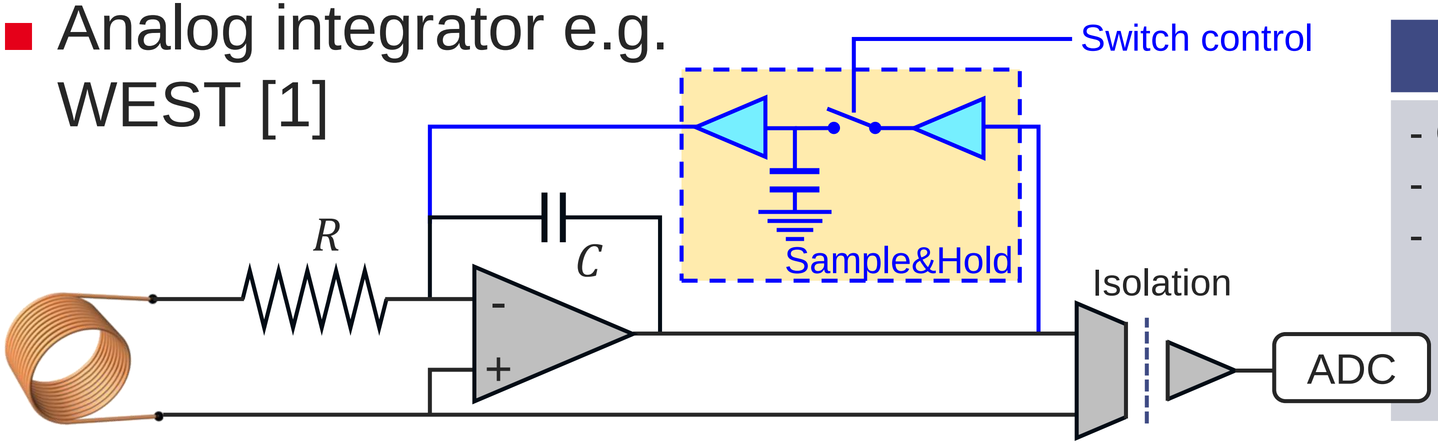

Advantage	Disadvantage
- Continuous output signal - Robust, Cheap (300 €) - No further processing	- Dynamic range limited to output stage - Special care during assembly and circuit selection - Special care for tuning

- Digital chopper integrator e.g. W7-X [2], ITER [3]

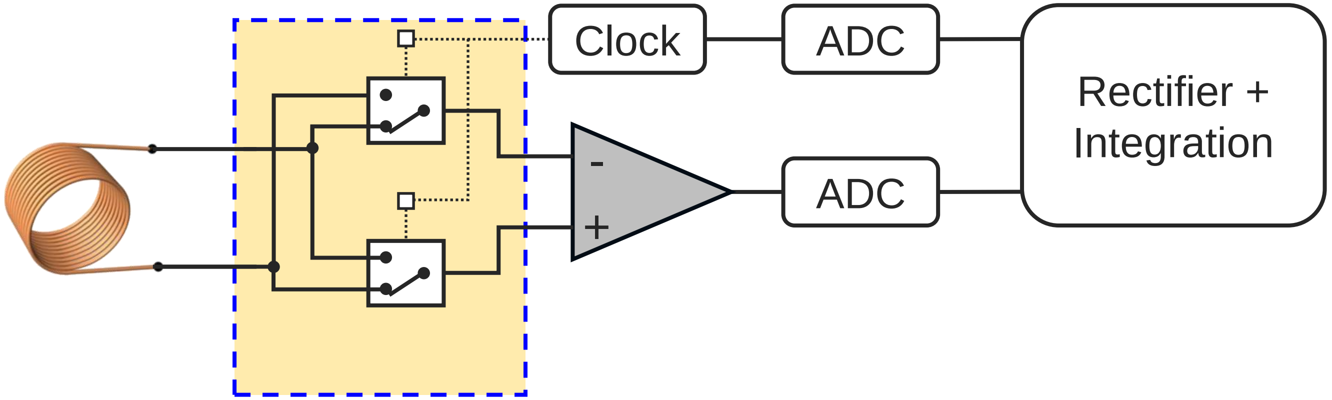

Advantage	Disadvantage
- Latency of the signal - Better control of drift and common mode - High dynamic range (up to 1000 V)	- Implementation is more complex - More expensive (~1 k€) - Requires further processing to obtain the integrated signal

[1] P. Spuig et al. Fusion Engineering and Design 96–97 (2015) 966–969; [2] A. Werner RSI **77** 10E307 (2006); [3] A. Batista Fusion Engineering and Design 123 (2017) 1025–1028

Which quantities to qualify the integrator performance?

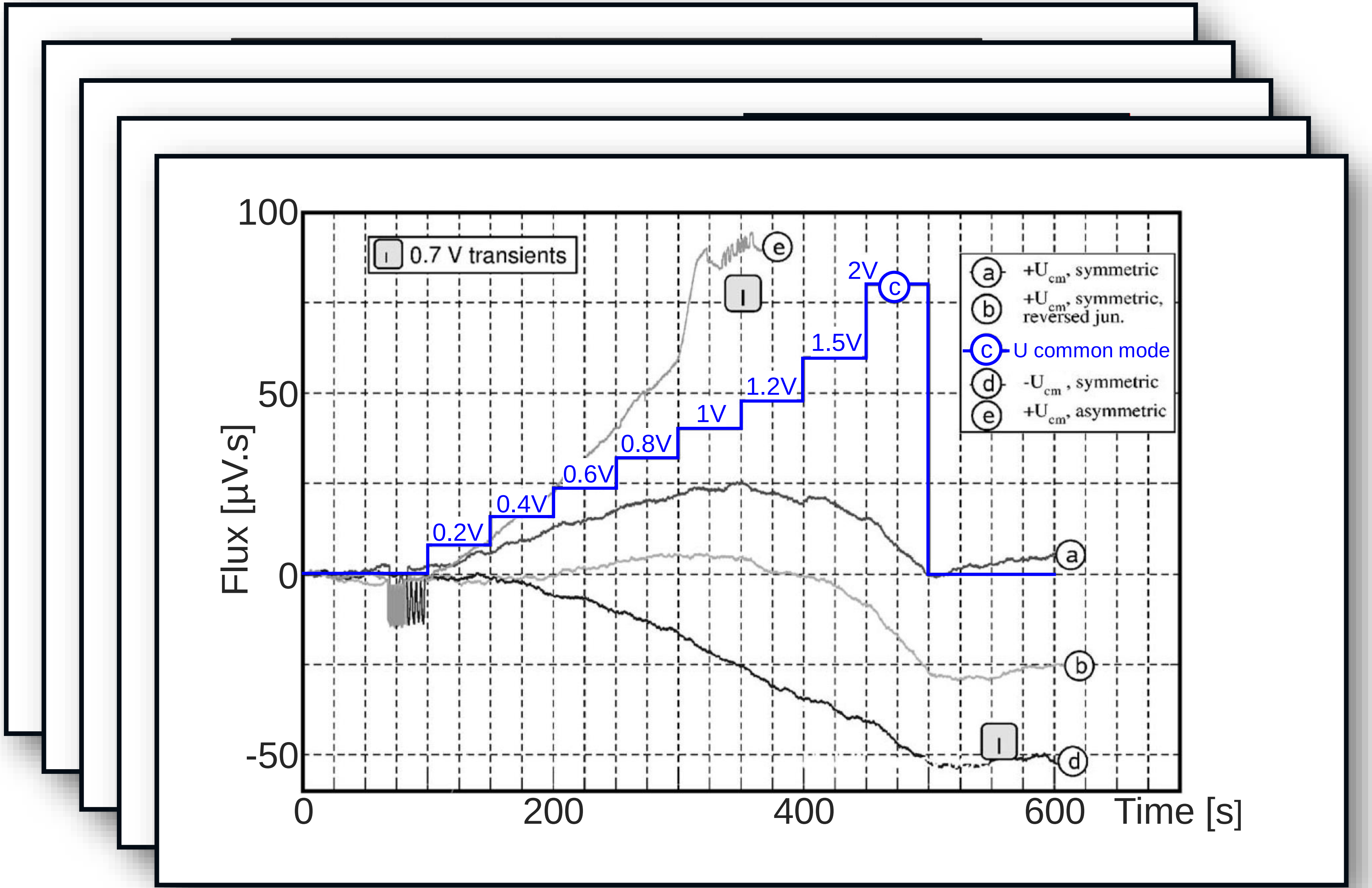

- Drift (ITER spec < 400 µV.s)
- Voltage standing
- Time constant and linearity
- Pulse response (Slew rate)
- CMRR (Common Mode Rejection Ratio) ITER spec > 140 dB

5. Equilibrium reconstruction, Real-Time data processing

[1] G. de Tommasi Magnetic equilibrium and instability control IIS 2022

The Grad-Shafranov equation

- Plasma equilibrium: force balance equation: $\vec{\nabla} p = \vec{j} \times \vec{B}$

  Plasma kinetic pressure — Magnetic pressure

- $\Rightarrow \vec{B} \cdot \vec{\nabla} p = 0$ and $\vec{j} \cdot \vec{\nabla} p = 0 \Rightarrow \vec{B}$ and $\vec{j}$ are lying on isobaric surfaces
- Iso-B surfaces coincide with iso-flux surfaces: $\vec{B} \cdot \vec{\nabla} \psi = 0$ ψ is poloidal flux function

- Grad-Shafranov equation: $$\boxed{\Delta^* \psi = -\mu_0 R^2 p'(\psi) - f(\psi) f'(\psi)}$$

With: $\Delta^* = R \frac{\partial}{\partial R} \frac{1}{R} \frac{\partial}{\partial R} + \frac{\partial^2}{\partial Z^2}$

$f(\psi) = R B_\varphi = \frac{\mu_0}{2\pi} I_{pol}(\psi)$ the poloidal current flux function ; $f'(\psi) = \frac{\partial f}{\partial \psi}$

$p(\psi)$ Plasma kinetic pressure; $p'(\psi) = \frac{\partial p}{\partial \psi}$

- Link to magnetic diagnostics: ψ flux measured with flux loops; $\vec{B}_R = -\frac{1}{R} \frac{\partial \psi}{\partial Z}$; $\vec{B}_Z = +\frac{1}{R} \frac{\partial \psi}{\partial R}$

Basic measurements: Plasma current centroid

- Plasma geometric properties can be estimated from magnetic meas. outside plasma [1]

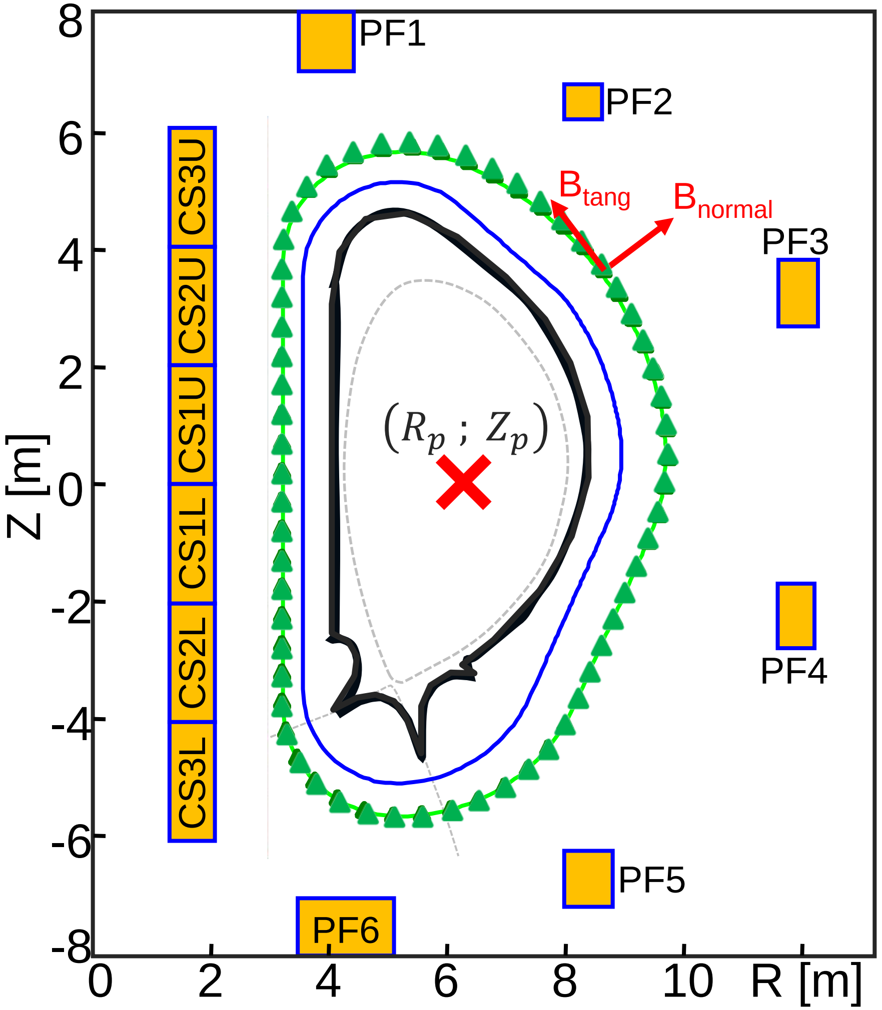

- Moment of the current distribution [1,2]

$$\iint f\, j_\varphi\, dS = \frac{1}{\mu_0} \oint f\, B_{tang} + R\, g\, B_{norm}\ dl$$

f is a solution of Grad-Shafranov eq., g is the conjugate fct of f.

- <u>Moment order 0:</u>

$$I_p = \iint j_\varphi\, dS = \frac{1}{\mu_0} \oint B_{tang}\, dl$$

- <u>Moment order 1:</u>

$$Z_p\ I_p = \iint Z_p\, j_\varphi\, dS = \frac{1}{\mu_0} \oint Z\, B_{tang} + R\, log\left(\frac{R}{R_0}\right) B_{norm}\ dl$$

- <u>Moment order 2:</u>

$$R_p^2\ I_p = \iint R_p^2\, j_\varphi\, dS = \frac{1}{\mu_0} \oint R^2\ B_{tang} + 2\, R\, Z\, B_{norm}\ dl$$

$(R; Z) =$ Sensor position; $(R_p; Z_p) =$ plasma position

[1] L.E. Zakharov, V.D. Shafranov, Equilibrium of a Toroidal Plasma with Noncircular Cross Section, Technical Report, IV Kurchatov Institute of Atomic Energy, Moscow, 1973.
[2] M. F. Reusch, G. Hutchinson, Finite Order Polynomial Moment Solutions of the Homogeneous Grad-Shafranov Equation, Tec. report, Princeton Univ., NJ (USA). 1984.

Outside the plasma: the plasma boundary (1/2)

- Grad-Shafranov equation is written as: $\boxed{\Delta^*\psi = 0}$ $(p = 0 \text{ and } I_{pol} = 0)$

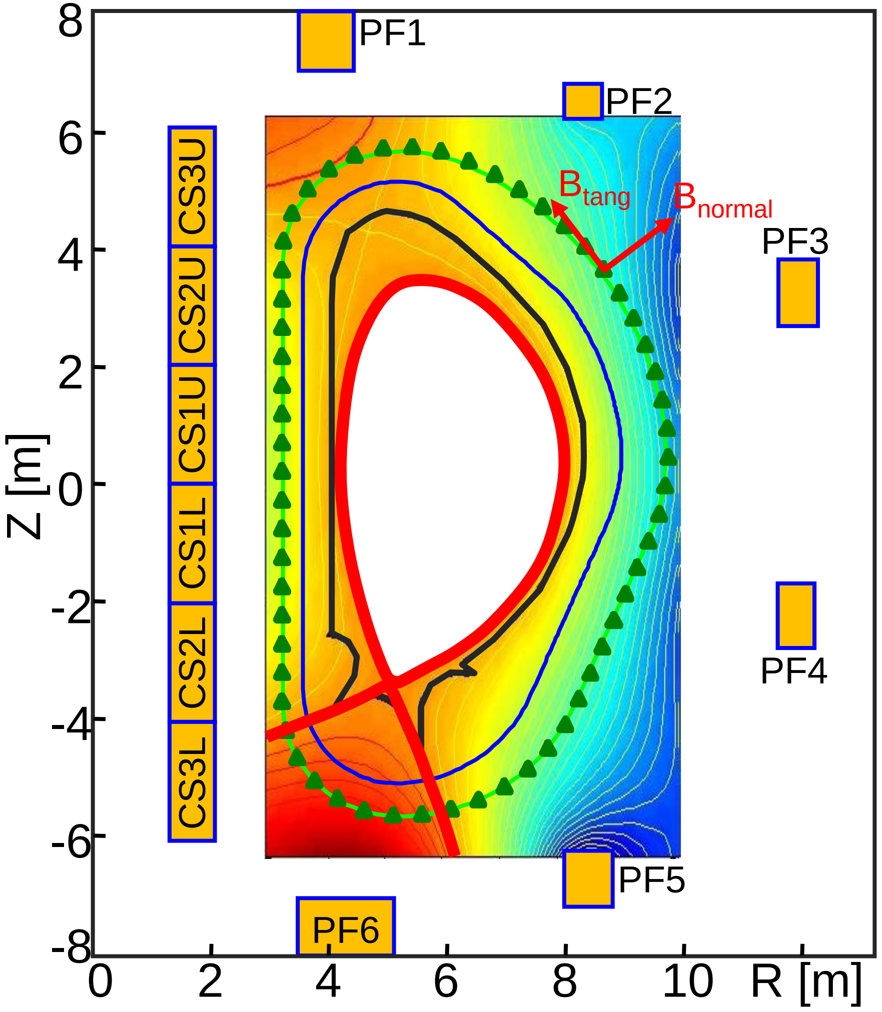

- Principle of reconstruction:
  1. **Approximate $\psi(R, Z)$ on the basis of measurements**
  2. Determine ψ_{Bnd} at the plasma boundary (X-point if any)
  3. Determine plasma boundary (ψ_{Bnd} isoflux)
  4. Calculate main plasma parameters

- Main issue is item#1,

- Pb: solve: $\Delta^*\psi = 0$
  inputs: magnetic diagnostics + PF/CS currents
  output: flux map outside the plasma

- Not a unique solution → ill posed problem

Outside the plasma: the plasma boundary (2/2)

- Grad-Shafranov equation is written as: $\boxed{\boldsymbol{\Delta^*\psi = 0}}$ ($p = 0$ and $I_{pol} = 0$)

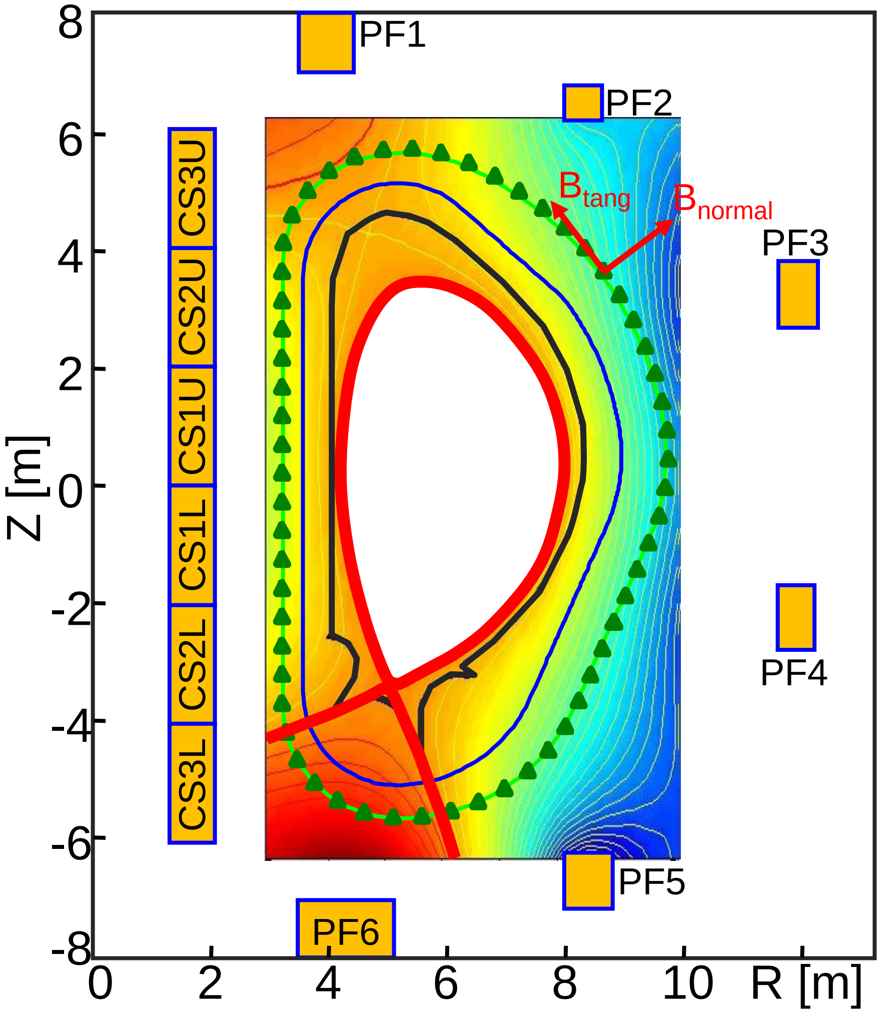

- Develop ψ on eigenfunctions basis ψ_k: $\tilde{\psi} = \sum_{k=0}^{m} c_k\, \psi_k$
- Solve pb of type: $\begin{bmatrix} [\psi(R,Z)] \\ [\partial\psi/\partial Z] \\ [\partial\psi/\partial R] \end{bmatrix} [c_k] = \begin{bmatrix} [\psi_{meas}] \\ [B_R] \\ [B_Z] \end{bmatrix}$

  10-20 parameters to determine; ~100 measures
  → Least square solution
- Several eigenfunctions bases can be used
  - natural choice = toroidal harmonics
  - Filament method: consider a set of filament inside plasma + Green's functions. Solve similar matrix pb
  - Hermit spline, etc.
- Neural network methods exist (need training)
- Application: RT plasma control, time cycle ~1 ms

Outside/Inside the plasma: non homogeneous Grad-Shafranov equation

- Grad-Shafranov equation is written as: $\Delta^* \psi = -\mu_0 R^2 p'(\psi) - f(\psi) f'(\psi)$

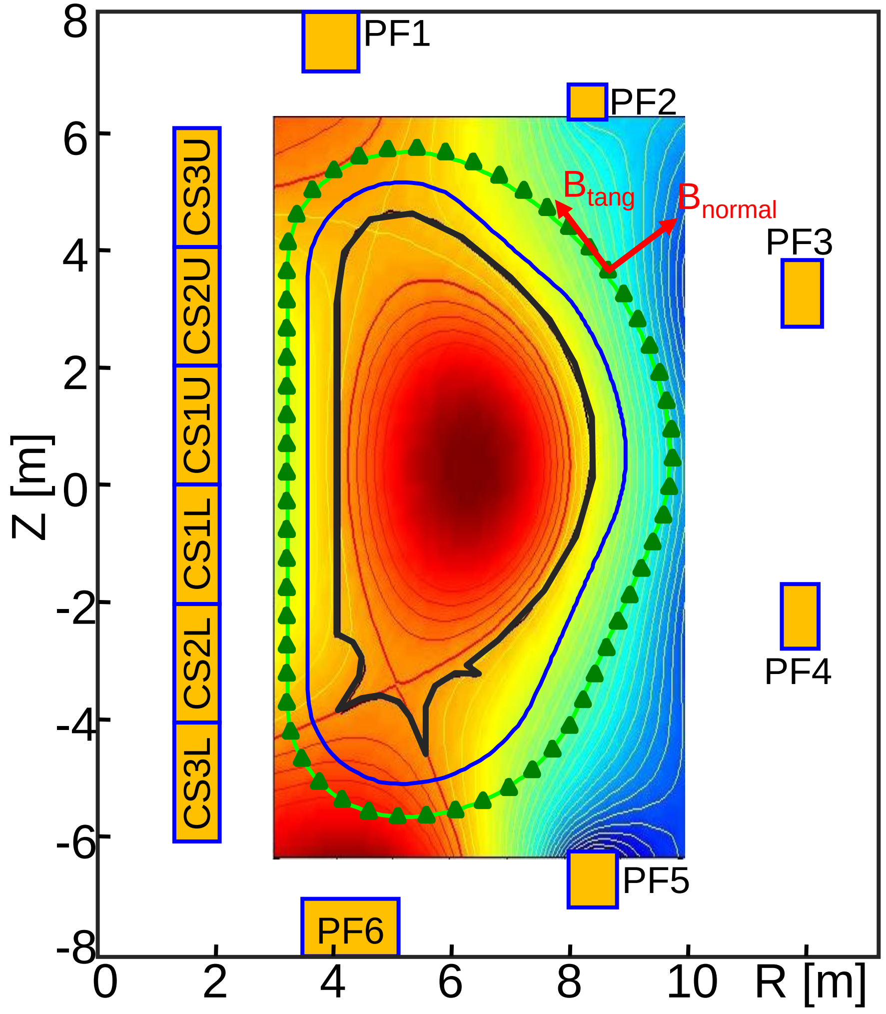

- Solve least square pb with additional constraints:
  - Current profile → $f(\psi)$ function
  - Pressure profile → $p(\psi)$ function
- Using only magnetic diagnostics inputs: $f(\psi)$ and $p(\psi)$ functions approximated by polynom (few parameters)
- Use additional inputs to constrain $f(\psi)$ and $p(\psi)$ profiles
  - e.g. MSE, polarimetry, etc. → $f(\psi)$
  - e.g. Thomson Scattering, XICS, etc. → $p(\psi)$
- Application: advanced RT control, time cycle 10-50 ms
- *Note: No need to have the full equilibrium to control the plasma pos&shape*

Plasma control: the role of magnetic diagnostics

Reference

I_p; R_p; Z_p; R_{Xpt}; Z_{Xpt}; plasma boundary; etc.

Plasma Control

PID or more advanced controllers

Actuators

CS, PF coils, H&CD, fueling

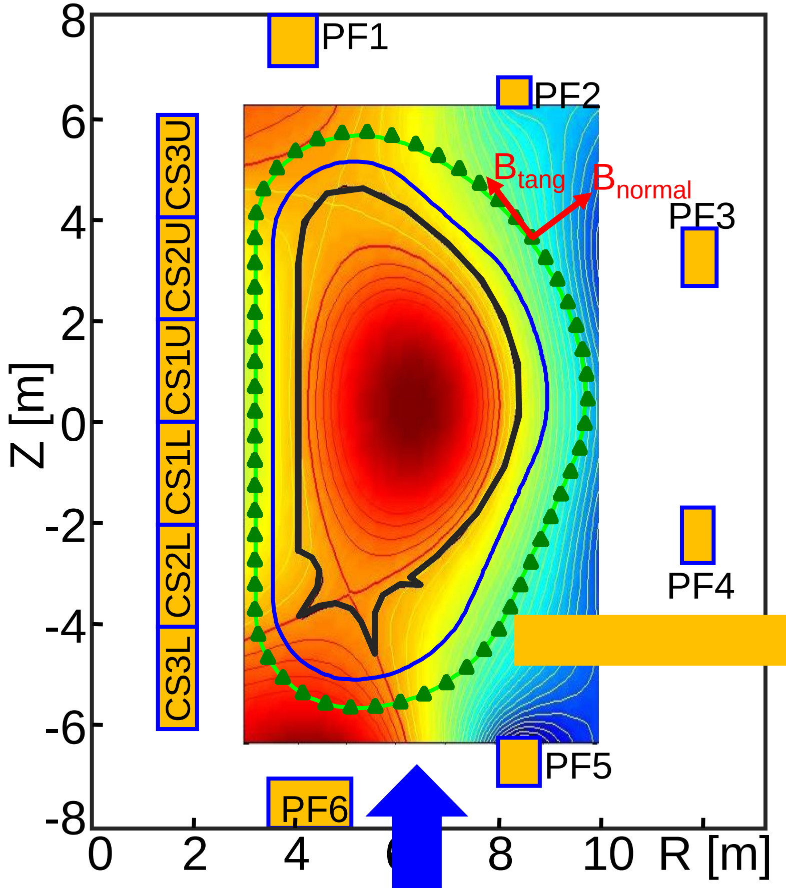

Magnetic diagnostics:

ψ; B_{norm}; B_{tang} outside plasma

Data processing:

I_p; R_p; Z_p; R_{Xpt}; Z_{Xpt}; plasma boundary; etc.

Solve $\Delta^*\psi$ equation

- Full cycle: ~1 ms

Short list of basic information obtained with magnetic diagnostics

Plasma current and loop voltage: $I_p = \frac{1}{\mu_0} \oint B_{tang}\, dl \qquad V_{loop} = \frac{\partial\, \psi_{plas}}{\partial\, t}$

Geometry

- Geom: $R_{Geom} = \frac{R_{in}+R_{out}}{2}$; $Z_{Geom} = \frac{Z_{up}+Z_{down}}{2}$; $a_p = \frac{R_{out}-R_{in}}{2}$; $A = \frac{R_{Geom}}{a_p}$
- elongation: $\kappa = b/a$
- triangularity: $\delta_{up} = b/a$
- Perimeter: $\Gamma = \sum dl_i = \sum (R_{i+1} - R_i)^2 + (Z_{i+1} - Z_i)^2$
- Surface: $S = 2\pi \sum (R_{i+1} - R_i)^2 dl_i/2$
- Poloidal area: $A = \sum (Z_{i+1} - Z_i)(R_{i+1} + R_i)/2$
- Volume: $V = 2\pi\, \langle R \rangle\, A$

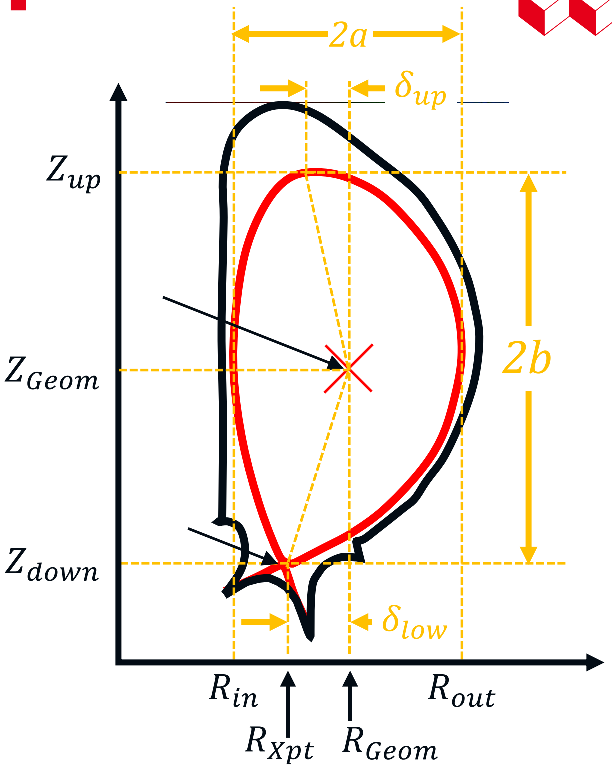

and much more …

- Shafranov parameters
  - $S_1 = \frac{1}{V\, B_{pa}^2} \iint_\Gamma B_{pol}^2 \left[(R - R_o)\, \overrightarrow{e_R} + Z\, \overrightarrow{e_Z} \right] \cdot \vec{n}\, dS$; $S_2 = \frac{1}{V\, B_{pa}^2} \iint_\Gamma B_{pol}^2 \langle R \rangle\, \overrightarrow{e_R} \cdot \vec{n}\, dS$; $S_3 = \frac{1}{V\, B_{pa}^2} \iint_\Gamma B_{pol}^2 \langle Z \rangle\, \overrightarrow{e_Z} \cdot \vec{n}\, dS$
  - $\beta + \frac{l_i}{2} = \frac{S_1}{2} + \frac{S_2}{2}\left(1 + \frac{R_{magAxis}}{\langle R \rangle}\right)$
  - $l_i = \frac{1}{\alpha - 1}\left(S_1 + S_2\left(1 - \frac{R_{magAxis}}{\langle R \rangle}\right) - 2S_3\right)$; $\alpha = 2 \iint_\Gamma \left(\overrightarrow{B_{pol}} \cdot \overrightarrow{e_Z}\right)^2 dS \,/ \iint_\Gamma B_{pol}^2\, dS$
- Diamagnetic parameters
  - $\mu = \frac{8\pi B_{\varphi 0}}{\mu_0^2\, I_p^2} \Delta\phi_{diam}$; $\beta_p = 1 - \mu$; $\beta_{dia} = S_1 + \left(1 - \frac{R_{magAxis}}{\langle R \rangle}\right) S_2 + \mu$; $W_{dia} = \frac{3}{8} \mu_0 \langle R \rangle I_p^2 \beta_{dia}$; etc.

Basic principle of low freq. MHD modes identification

- Signal on a MHD sensor:

$$S_{MHD} = \sum_{m,n} A_{m,n}\, exp\big[j\,(\omega_{m,n}t + m\theta + n\varphi)\big]$$

- Phase shift between sensors

$$\delta\phi_{sensor} = n\varphi + m\theta'$$

$$\theta' = \theta + \lambda\, sin(\theta) \qquad \lambda = \frac{R_p}{a_p} + \frac{D_0}{2\, a_p}$$

- Identify m and n using several MHD sensors

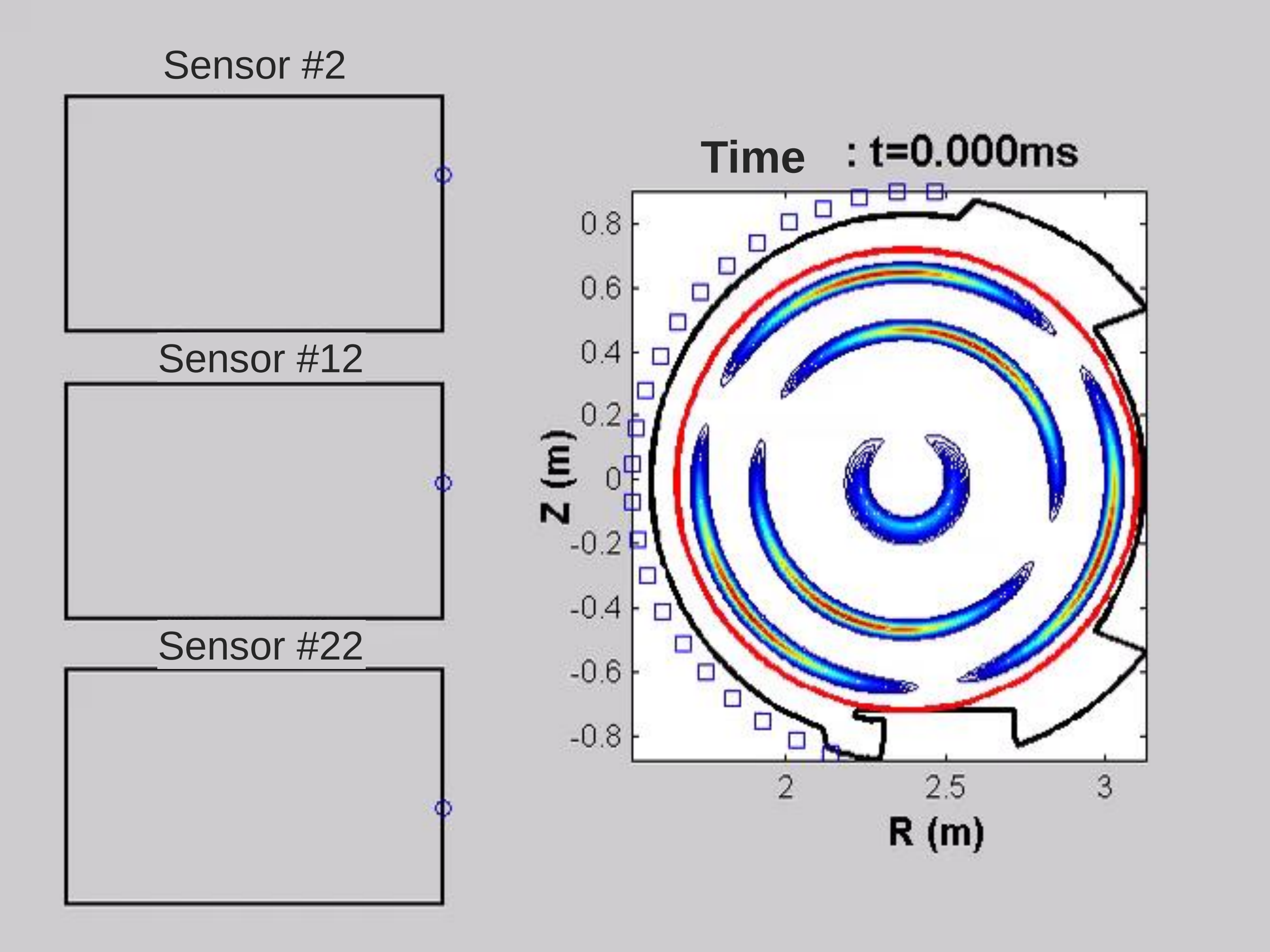

Basic principle of low freq. MHD modes identification

- Signal on a MHD sensor:

$$S_{MHD} = \sum_{m,n} A_{m,n}\, exp[j\,(\omega_{m,n} t + m\theta + n\varphi)]$$

- Phase shift between sensors

$$\delta\phi_{sensor} = n\varphi + m\theta'$$

$$\theta' = \theta + \lambda\, sin(\theta) \qquad \lambda = \frac{R_p}{a_p} + \frac{D_0}{2\, a_p}$$

- Identify m and n using several MHD sensors

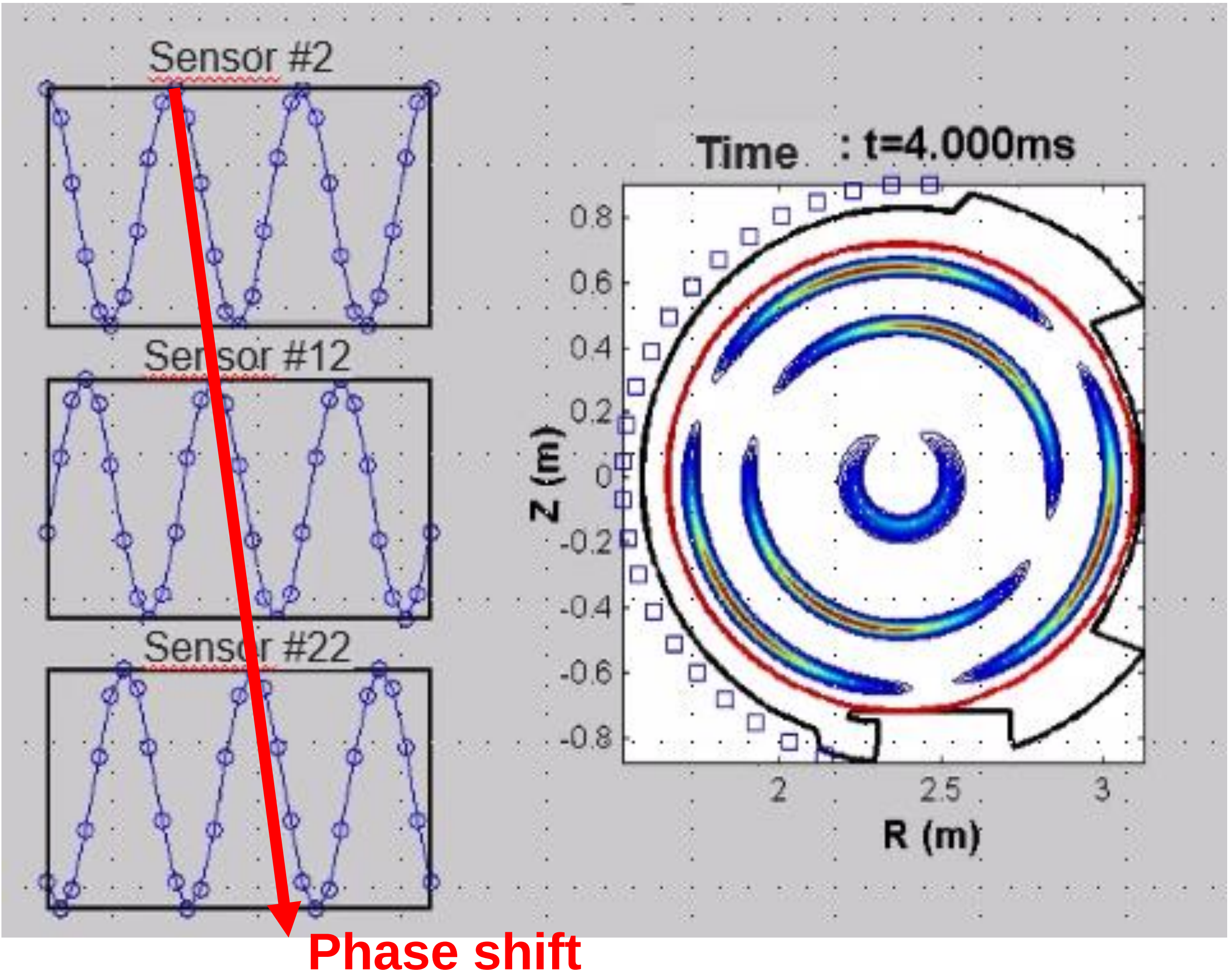

Example of plasma discharge

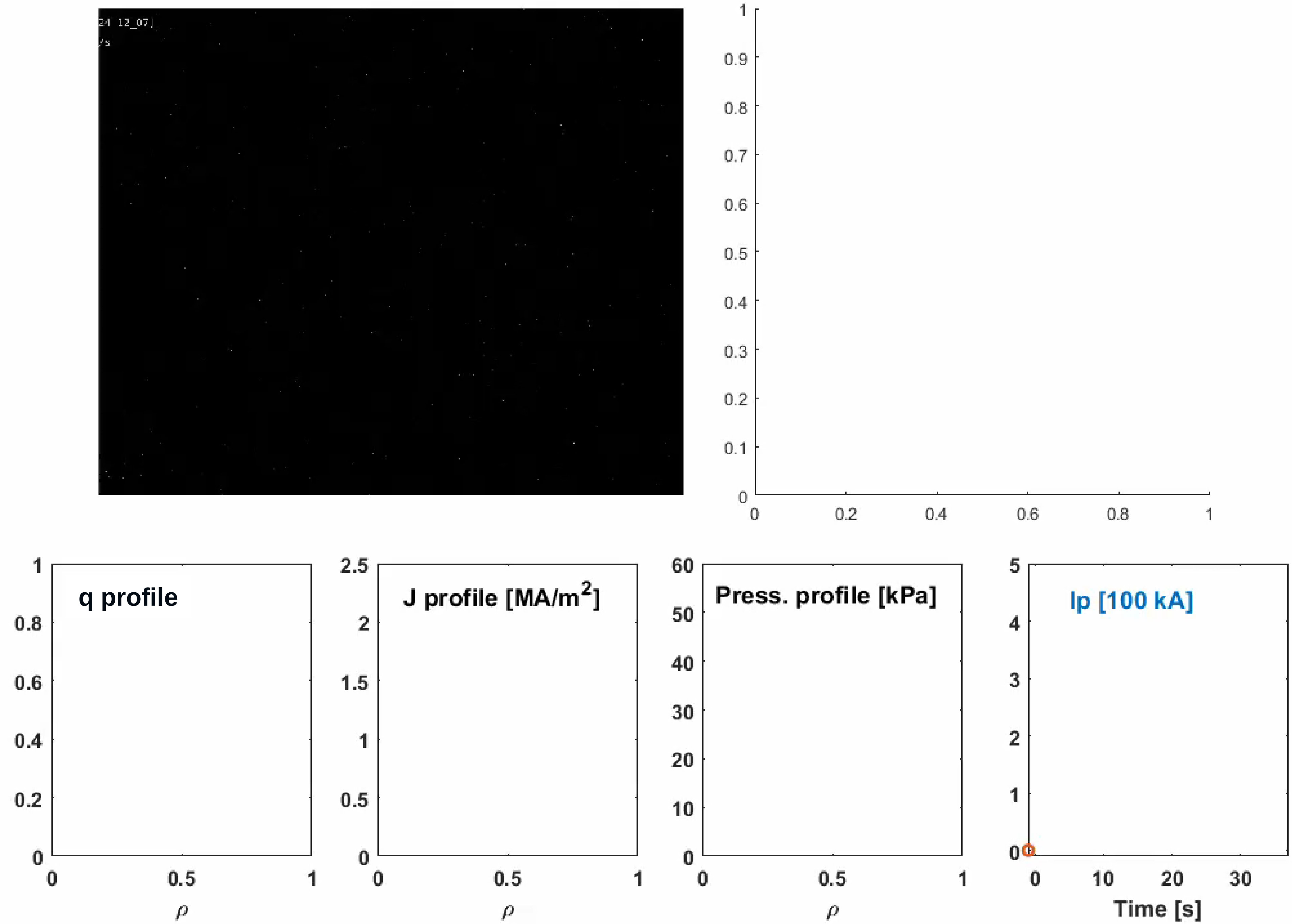

Thank you for your attention

philippe.jacques.moreau@cea.fr

■ Bibliography

Bibliography (1/3)

- **Books:**
  - Alan Wootton “Magnetic Fields and Magnetic Diagnostics for Tokamak Plasmas”
  - M. Ariola, A. Pironti “Magnetic Control of Tokamak plasmas”, Springer

- **General overview:**
  - Evangéline Benevent “Magnetic sensors”
  - H. Weisen, EPFL doctoral course: “Diagnostics of magnetically confined fusion plasmas”
  - M. Urbaniak, Basic magnetic measurement methods”, lecture
  - J.E. Lenz, “A review of magnetic sensors”, PROCEEDINGS OF THE IEEE, VOL. 78, NO. 6, JUNE 1990
  - K. Makishima, Measuring Magnetic Fields of Neutron Stars, Progress of Theoretical Physics Supplement No. 151, 2003

- **Integrators:**
  - J.D. Broesch et al. “A digital long pulse integrator”, IEEE (1995)
  - Y. Wang et al. “A digital long pulse integrator for EAST tokamak”, Fus. Eng. and design, **89**, (2014)
  - Y. Wang et al. “A New Analog Integrator for Magnetic Diagnostics on EAST”, IEEE transactions on nuclear science, **66**,. 7, July 2019
  - A.J.N Batista et al., “F4E prototype of a chopper digital integrator for the ITER magnetics”, Fus Eng. and design **123** (2017)
  - A.J.N Batista et al., “Testing results of chopper based integrator prototypes for the ITER magnetics”, Fus Eng. and design **128** (2018)
  - K. Kurihara et al. “Development of a Precise Long-Time Digital Integrator for Magnetic Measurements in a Tokamak”, IEEE (1998)
  - E.J. Strait et al. “A hybrid digital–analog long pulse integrator”, Rev. Sci. Instrum. 68, 381–384 (1997)
  - S. Ali Arshad et al. “Long - pulse analog integration”, Rev. Sci. Instrum. 64, 2679–2682 (1993)
  - A. Werner et al. “W7-X magnetic diagnostics: Performance of the digital integrator”, Rev. Sci. Instrum. 77, 10E307 (2006)
  - P. Spuig et al. “Enhanced integrators for WEST magnetic diagnostics”, Fus. Eng. and design **96-97** (2015)

Bibliography (2/3)

- **Neutron effects:**
  - L. Vermeeren, "Neutron irradiation and temperature effects on induced voltages in MI and ceramic-coated cables as a function of temperature", EFDA-reference: TW6-TPDC-IRRCER-D4.2, Dec. 2008
  - L. Vermeeren, "Temperature effects on induced voltages in MI and ceramic-coated cables", EFDA: TW6-TPDC-IRRCER-D4.2, Oct. 2007
  - R. Van Nieuwenhove et al., "Study of the RIEMF effect on mineral insulated cables for magnetic diagnostics in ITER", Fus. Eng. and Design 66-68C, 821-825 (2003)
  - L. Vermeeren et al., "Theoretical study of radiation induced electromotive effects on MI cables", Rev. Sci. Instr. 74, 4667-4674 (2003)
  - R. Van Nieuwenhove et al., "Experimental study of radiation induced electromotive effects on MI cables", Rev. Sci. Instr. 74, (2003)
  - T. Nishitani et al., "Radiation-induced thermoelectric sensitivity in the MI cable of magnetic diagnostic coils for ITER", J. Nucl. Mat. 329-333, 1461-1465 (2004)
  - L. Vermeeren et al., "Induced voltages and currents in copper and stainless steel core mineral insulated cables due to radiation and thermal gradients", Fusion Engineering and Design 82, 5-14, 1185-1191 (2007)
  - R. Vila et al. "RIEMF in MgO and Al2O3 insulated MI cable ITER magnetic diagnostic coils", Journal of Nuclear Materials 329–333 (2004)
  - G. Vayakis et al., "Radiation-induced thermoelectric sensitivity (RITES) in ITER prototype magnetic sensors", Rev. Sci. Instrum. **75**, (2004)

- **ITER:**
  - S.Entler, Development of the ITER steady-state magnetic field sensors
  - Y. Ma et al. Design and development of ITER high-frequency magnetic sensor, Fusion Engineering and Design **112**, Nov. 2016, 594-612
  - G. Vayakis et al. "Magnetic diagnostics for ITER/BPX plasmas", Rev. Sci. Instrum. **74**, 2409–2417 (2003)
  - D. Testa et al. "The Magnetic Diagnostic Set for ITER", IEEE transactions on plasma science, vol. 38, no. 3, March 2010
  - E.J. Strait et al. "Chapter 2: Magnetic Diagnostics", Fusion Science and Technology, 53:2, 304-334
  - A.J.H. Donné et al. "Chapter 7: Diagnostics", Nucl. Fusion 47 (2007) S337–S384
  - G. Vayakis et al. "Chapter 12: Generic Diagnostic Issues for a Burning Plasma Experiment", Fusion Science and Technology, 53:2, 699-750

Bibliography (3/3)

- **Plasma Control:**
  - Gianmaria de Tommasi, “Magnetic equilibrium and instability control”, IIS 2022

- **Real time equilibrium reconstruction:**
  - L.L. Lao et al. “Reconstruction of current profile parameters and plasma shapes in tokamaks”, Nucl. Fusion **25** 1611 (1985)
  - K. Kurihara 1993 Tokamak plasma shape identification on the basis of boundary integral equations, Nucl. Fusion **33** 399
  - K. Kurihara et al. “A new shape reproduction method based on the Cauchy-condition surface for real-time tokamak reactor control”, Fud. Eng. and design **51-52** (2000)
  - J.R. Ferron et al, “Real time equilibrium reconstruction for tokamak discharge control” 1998 Nucl. Fusion **38** 1055
  - D.P. O'Brien et al 1993, “Local expansion method for fast plasma boundary identification in JET”, Nucl. Fusion **33** 467
  - B.J. Braams et al., Fast determination of plasma parameters through function parametrization 1986 Nucl. Fusion **26** 699
  - F. Hofmann et al., Fast identification of plasma boundary and Xpoints in elongated tokamaks 1988 Nucl. Fusion **28** 519
  - J.B. et al. Fast non-linear extraction of plasma equilibrium parameters using a neural network mapping, 1991 Nucl. Fusion 31 1291
  - D.W. Swain et al. An efficient technique for magnetic analysis of non-circular, high-beta tokamak equilibria1982 Nucl. Fusion 22 1015
  - B. Faugeras et al. Tokamak plasma boundary reconstruction using toroidal harmonics and an optimal control method, Fusion Science and Technology, 2016, 69 (2), pp.495-504
  - W. Schneider et al. “ASDEX Upgrade MHD equilibria reconstruction on distributed workstations”, Fus Eng and Design **48** (2000)
  - L Giannone et al. Magnetics only real-time equilibrium reconstruction on ASDEX Upgrade”, Plasma Phys. Control. Fusion 66 (2024)
  - S. Tsaun et al. Real-time plasma boundary reconstruction in the KSTAR tokamak using finite element method, Fus Eng and Design **82** (2007) 163–174